iScience

CellPress
OPEN ACCESS

Article

Electrochemical ammonium-cation-assisted pyridylation of inert N-heterocycles via dual-proton-coupled electron transfer

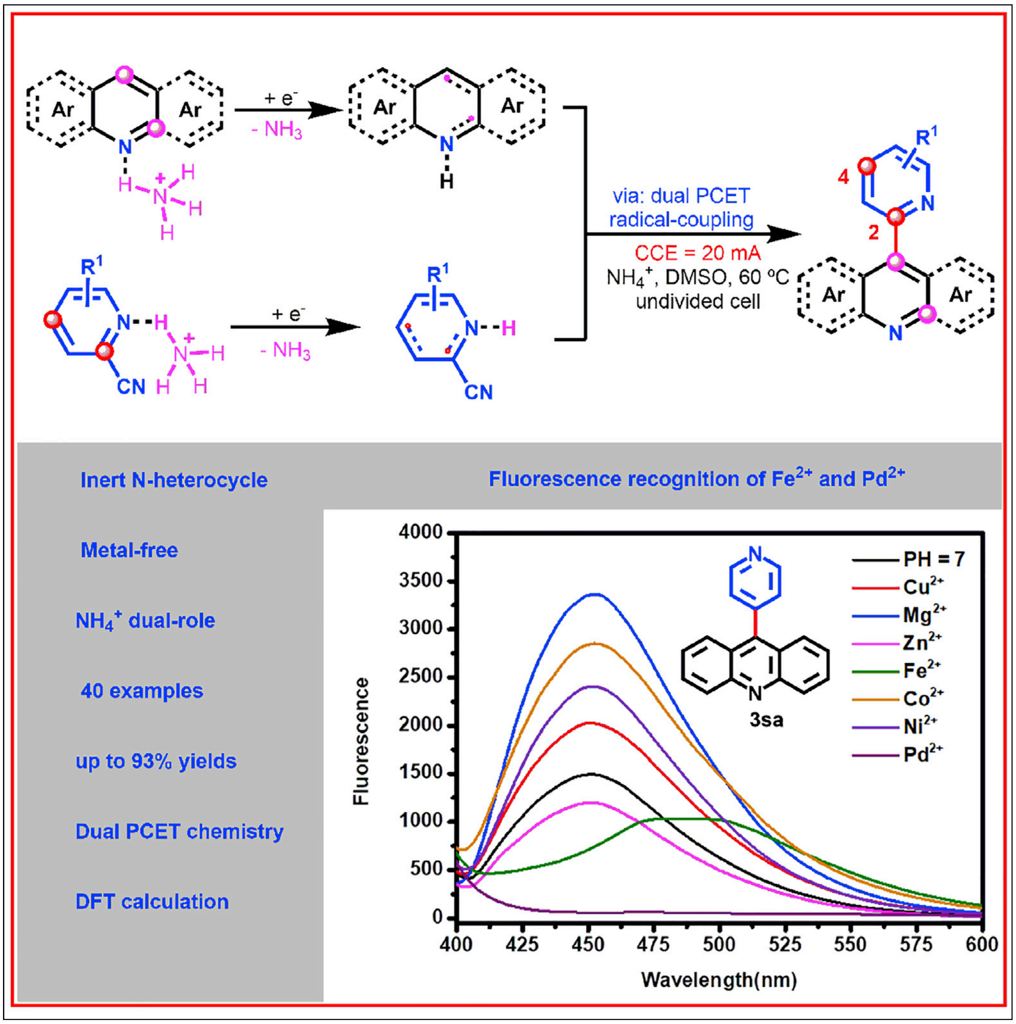

Cong Niu, Jianjing Yang, Kelu Yan, Jiafang Xie, Wei Jiang, Bingwen Li, Jiangwei Wen

wenjy@qfnu.edu.cn

Highlights

Electrochemical NH_4^+-assisted dual PCET followed by the radical cross-coupling

Straightforward and practical synthetic route for N-fused heterocycles

Fluorescence recognition of Fe^{2+} and Pd^{2+} with high-sensitivity

Niu et al., iScience *25*, 104253
May 20, 2022
https://doi.org/10.1016/j.isci.2022.104253

iScience

CellPress OPEN ACCESS

Article

Electrochemical ammonium-cation-assisted pyridylation of inert N-heterocycles via dual-proton-coupled electron transfer

Cong Niu,[1,3] Jianjing Yang,[1,3] Kelu Yan,[1] Jiafang Xie,[1] Wei Jiang,[1] Bingwen Li,[2] and Jiangwei Wen[1,4,*]

SUMMARY

A straightforward and practical strategy for pyridylation of inert N-heterocycles, enabled by ammonium cation and electrochemical, has been described. This protocol gives access to various N-fused heterocycles and bidentate nitrogen ligand compounds, through dual-proton-coupled electron transfer (PCET) and radical cross-coupling in the absence of exogenous metal and redox reagent. It features broad substrate scope, wide functional group tolerance, and easy gram-scale synthesis. Various experiments and density functional theory (DFT) calculation results show the mechanism of dual PCET followed by radical cross-coupling is the preferred pathway. Moreover, ammonium salt plays the dual role of protonation reagent and electrolyte in this conversion, and the resulting product 9-(pyridin-4-yl)acridine compound can be used for fluorescence recognition of Fe^{2+} and Pd^{2+} with high sensitivity.

INTRODUCTION

Pyridines are among the most representative heterocycles in pharmaceuticals, materials, natural product molecules, and organic functional materials (Yadav and Reddy, 2003, Chen et al., 2006; Moser et al., 2008; Misale et al., 2012; Afeli et al., 2013; Felding et al., 2014; Kouznetsov et al., 2017; Gil-Martins et al., 2020). As a result, new methods for the construction of functionalized pyridines from abundant precursors are an important synthetic goal (Nakao, 2011; Murakami et al., 2017; Wang et al., 2021, Zhou and Jiao, 2021). It is considered a straightforward and challenging protocol to access biologically active N-heterocyclic compounds from the inert N-heterocycles with cyanopyridine derivatives via the mechanism of radical cross-coupling reaction (Scheme 1A) (Proctor and Phipps, 2019; Bordi and Starr, 2017; Dong et al., 2021, Jin and MacMillan, 2015; Li, 2009; Ma et al., 2017, Wang et al., 2017). It is well known that electron-deficient pyridine derivatives are often modified into salts as radical acceptors for Minisci reactions due to their inherently negative electrode potential, which makes them difficult to activate (Scheme 1B) (Proctor and Phipps, 2019). The dual-proton-coupled electron transfer strategy may provide a promising roadmap for this transformation (Lehnherr et al., 2020; Murray et al., 2022; Tay et al., 2022). Although various elegant pyridylation strategies have been established in recent years by employing photocatalysis and metal or metal-free catalysis (Huang et al., 2021; Kim et al., 2019; Novaes et al., 2021; Shen et al., 2021; Tong et al., 2021; Xu et al., 2021; Zhang et al., 2017a, 2017b, 2020, 2021; Zhu et al., 2019). However, the pyridylation of inert N-heterocyclic derivatives via dual-proton-coupled electron transfer with radical cross-coupling in the absence of metals and external reducing agents under the conditions of electrochemical has not been reported (Wu et al., 2021; Zeng et al., 2021; Liu et al., 2018; Lu et al., 2022; Yuan et al., 2021; Chen et al., 2010; Zhao et al., 2006).

In recent years, multifarious important pyridine-containing functional molecules have been constructed based on the decyanation of cyanopyridines mediated by electrochemical reduction (Xu et al., 2021; Zhang et al., 2020, 2021; Lehnherr et al., 2020; Wen et al., 2021). Previously, we have delivered the C3 pyridylation of quinoxalin-2(1H)-ones with readily available cyanopyridines under the electrochemical conditions by employing HFIP as the protonation reagent (Scheme 1C) (Wen et al., 2021). However, we found that the pyridylation of electron-deficient quinolines cannot be achieved by adopting the previous protocol. Inspired by the mechanism of electrochemical ammonium cation-assisted ketone-activated alkene hydrogenation of pyridine to obtain β-pyridyl ketones (Yang et al., 2022). Herein, we developed the first straightforward and practical strategy for the pyridylation of electron-deficient quinolines aided by NH_4^+ in an

[1]Institute of Medicine and Materials Applied Technologies, College of Chemistry and Chemical Engineering, Qufu Normal University, Qufu, Shandong 273165, P. R. China

[2]Shandong Key Laboratory of Biophysics, Institute of Biophysics, Dezhou University, Dezhou 253023, P. R. China

[3]These authors contributed equally

[4]Lead contact

*Correspondence: wenjy@qfnu.edu.cn

https://doi.org/10.1016/j.isci.2022.104253

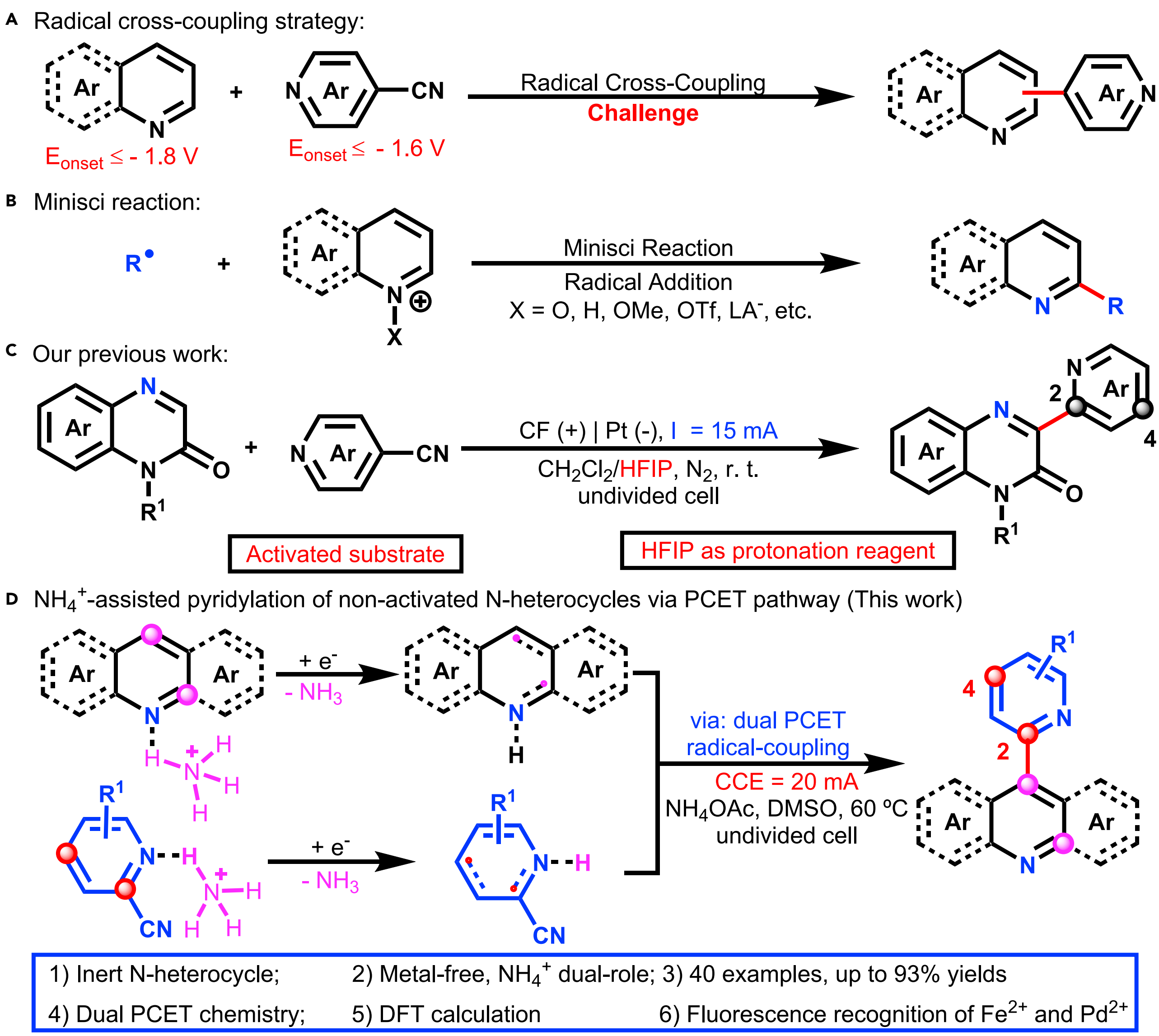

Scheme 1. Pyridation of N-heterocycles

(A) Radical cross-coupling strategy, (B) Minisci reaction, (C) Our previous work, (D) Pyridylation of N-heterocycles.

undivided cell via the dual PCET followed by the radical cross-coupling (Scheme 1D). All the experimental and DFT calculation results have disclosed that the mechanism of dual PCET and radical cross-coupling pathway is more reasonable. Interestingly, 9-(pyridin-4-yl)acridine compounds can be applied to the fluorescence recognition of Fe^{2+} and Pd^{2+} with high sensitivity.

RESULTS AND DISCUSSION

Optimization conditions

The electrochemical pyridylation of electron-deficient quinolines was selected as a benchmark (Table 1). Initially, 4-methylquinoline **1e** and 4-cyanopyridine **2a** were selected as the template coupling substrate to optimize the reaction conditions. By optimizing various reaction parameters, it was found that the desired product **3ea** was obtained in 88% isolated yield by performing the reaction under constant current electrolysis at 20 mA cm^{-2} in an undivided cell using NH_4OAc as the electrolyte and protonation reagent and two carbon rods as the working electrode and anode in CH_3CN/DMSO at 60°C for 5 h (Table 1, entry 1). Undoubtedly, the control experiments demonstrate that both electricity and NH_4^+ play a key role in this

Table 1. Optimization of the reaction conditions

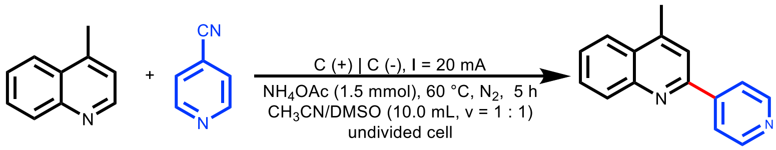

Entry	Deviation from standard conditions[a]	The yield of **3ea** (%) [b]
1	none	88
2	without current	n. d.
3	without NH_4OAc with $^nBu_4NBF_4$ as electrolyte	10
4	room temperature	65
5	NH_4I instead of NH_4OAc	66
6	NH_4Br instead of NH_4OAc	93
7	entry 1, but 1.0 mmol or 2.0 mmol of NH_4OAc	65, 80
8	entry 1, but 15 mA, or 25 mA	53, 84
9	without DMSO	4
10	DMF instead of DMSO	16
11	CH_2Cl_2 instead of CH_3CN	51
12	Pt (–) instead of C (–)	14
13	Pt (+) instead of C (+)	27

[a]Reaction conditions: carbon rods (φ = 6 mm) as the anode, carbon rods (φ = 6 mm) as the cathode, constant current 20 mA, **1d** (0.25 mmol), **2a** (0.75 mmol), NH_4OAc (1.5 mmol, 115.5 mg), CH_3CN/DMSO (1 : 1, v/v, 10.0 mL), 60°C, N_2, 5 h (14.9 $Fmol^{-1}$). "n. d." = not detected.
[b]Isolated yield.

transformation (Table 1, entries 2–3). Moving the reaction to ambient temperature caused the yield to fall from 88% to 65%, suggesting that adequate heating is more conducive to this conversion (Table 1, entry 4). To our delight, the desired product **3ea** can be delivered in 66% and 93% yields by employing NH_4I and NH_4Br as sources of ammonium cations (Table 1, entries 5–6). Besides, it was found that both increasing and decreasing the amount of NH_4OAc or the total charge was detrimental to the output of the desired product (Table 1, entries 7–8). Varying the mixed solvent of CH_3CN/DMSO also led to significantly lower yields (Table 1, entries 9–11). Finally, the effect of the electrode material was also investigated, and the reaction efficiency was lower when platinum plates were used in place of carbon rods as anode or cathode (Table 1, entries 12–13).

Mechanistic studies

Experimental studies

With the optimized conditions at hand, to better understand the mechanism of this reaction, various CV, ^1H NMR, and control experiments were preferentially carried out. Firstly, several CV and ^1H NMR experiments were performed to expound the role of NH_4^+ in the pyridylation of 4-methylquinoline (Figure 1). The reduction electrode potentials of **1e** and **2a** were preferentially recorded with E_{onset} = −1.86 V versus Ag/AgCl (Figure 1A, black line) and E_{onset} = −1.6 V versus Ag/AgCl (Figure 1B, black line), respectively.

To our delight, the electrode potentials of **1e** or **2a** were significantly decreased when the cyclic voltammetry experiments were scanned in NH_4OAc at a concentration of 1.5 mM, which is probably due to the effect of protonation (Figures 1A and 1B, red line). Based on the CV results, we speculate that the peaks of −0.98 V versus Ag/AgCl and 1.01V versus Ag/AgCl should be attributed to the reduction electrode potentials of **INT1** and **INT4**, respectively. Subsequently, we observed a significant positive shift in the reduction electrode potential of **1e** or **2a** with the increasing NH_4OAc concentration. These results are consistent with the PCET process in this reaction. Besides, a series of ^1H NMR experiments were designed and carried out to further verify the protonation of **1e** or **2a** with NH_4OAc. As shown in Figure 2, the hydrogen of NH_4^+ (5.91 ppm) was completely consumed in the presence of **1e** or **2a**, a broad peak at 6.28 ppm or 6.7 ppm was

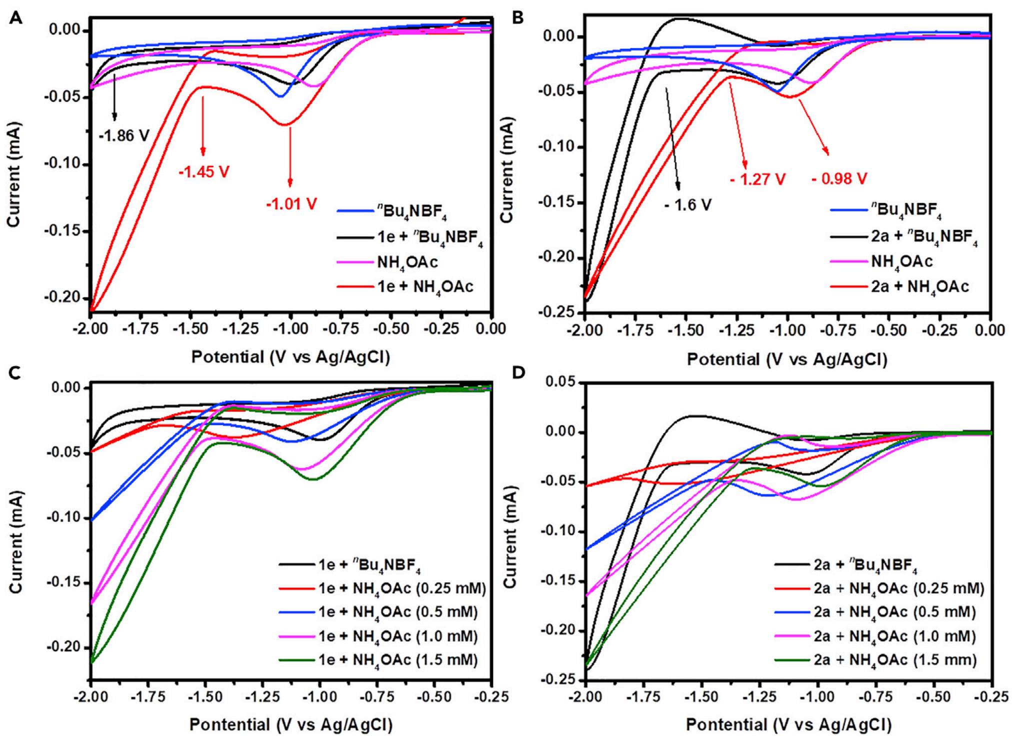

Figure 1. Cyclic Voltammetry experiments

(A–D) Cyclic Voltammetry at glass carbon as work electrode, Pt (1.5 × 1.5 cm^2) as counter electrode, Ag/AgCl (KCl), $^nBu_4NBF_4$ (0.1 M), CH_3CN/DMSO (1 : 1, v/v, 10.0 mL), scan rate 100 mV/s (A), (B) 1e (0.25 mM), 2a (0.25 mM), NH_4OAc (1.5 mM), (C), (D) CH_3CN/DMSO (1 : 1, v/v, 10.0 mL), 1e (0.25 mM), 2a (0.25 mM) with varying concentration of NH_4OAc, without $^nBu_4NBF_4$.

highlighted, and all of the chemical shifts were shifted to higher filed. These results further demonstrate that both **1e** and **2a** are readily protonated with NH_4^+ to generate pyridinium, which leads to the electrode potential of **1e** to drop from −1.86 V to −1.45 V versus Ag/AgCl and **2a** to drop from −1.61 V to −1.27 V versus Ag/AgCl. Moreover, the reduction electrode potentials of **1e** (E_{onset} = −1.45 V versus Ag/AgCl) and **2a** (E_{onset} = −1.27 V versus Ag/AgCl) in the presence of NH_4OAc were compared, and the result confirms that the protonated **2a** should be preferentially reduced on the surface of the cathode (Figure 3A).

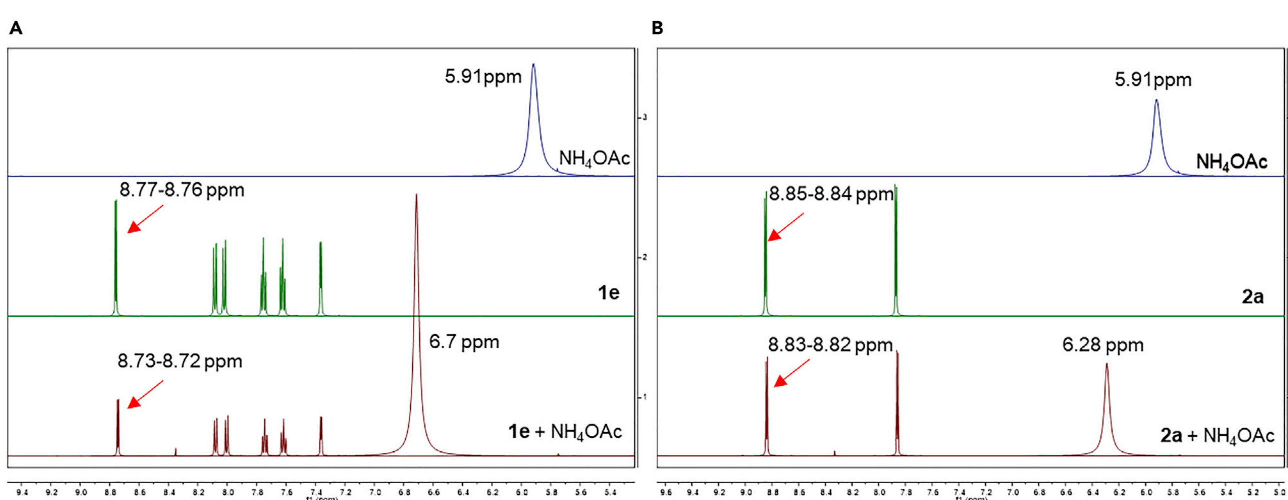

Figure 2. Comparison of ^1H NMR results in DMSO-d6, 1e or 2a/NH_4OAc = 1/8

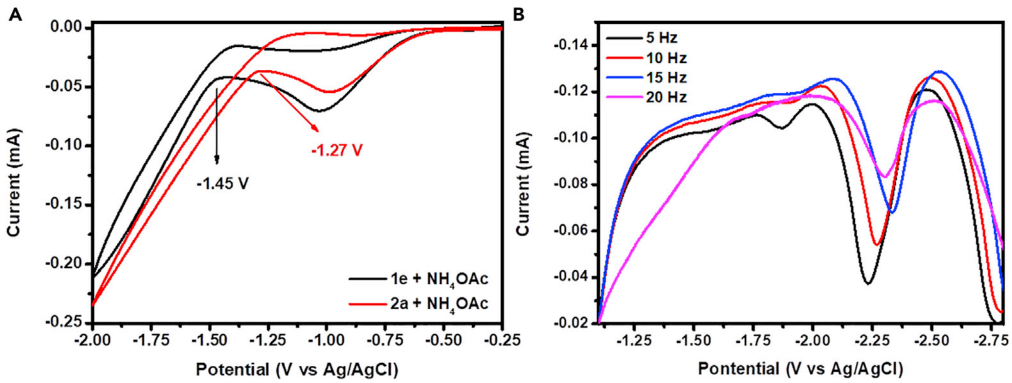

Figure 3. Cyclic Voltammetry at glass carbon as work electrode, Pt (1.5 × 1.5 cm^2) as counter electrode, Ag/AgCl (KCl), $^{n}Bu_4NBF_4$ (0.1 M), DMSO (10.0 mL)

(A) 1e (0.25 mM), 2a (0.25 mM), NH_4OAc (1.5 mM), scan rate 100 mV/s.

(B) Square wave voltammetry (SWV) was performed on solutions containing 0.1 M $^{n}Bu_4NBF_4$ in DMSO at room temperature in the presence NH_4OAc (1.5 mM), 1e (0.25 mM), 2a (0.5 mM), at a pulse height of 25 mV, step height of 4 mV, and with different of frequency.

Furthermore, the square-wave voltammetry (SWV) experiments of **1e** and **2a** were performed in the presence of NH_4OAc to further explore the electron transfer of the reaction mechanism (Figure 3B) (Yang et al., 2022; Peters et al., 2019; Liu et al., 2020). The peak splits significantly with the frequency change, which is consistent with the process of proton-coupled electron transfer. To our delight, the SWV results of the mixture of **1e** and **2a** indicate that this transformation should be performed by four-electron transfer (Figure 3B, black line, 5 Hz), which is consistent with the conclusion of the DFT calculation.

Next, various radical inhibition and potentiostatic electrolysis experiments were performed to gain insight into the details of the reaction mechanism (Scheme 2). First, the desired product **3ea** was almost suppressed when CBr_4 and 2,2,6,6-tetramethylpiperidin-1-oxyl (TEMPO) were employed as radical inhibitors, indicating that the mechanism of the radical process should be experienced in this transformation (Schemes 2A and 2B). Subsequently, a series of potentiostatic electrolysis experiments were carried out to verify our speculation on the reduction potential of **INT1** (−0.98 V versus Ag/AgCl) and **INT4** (−1.01V versus Ag/AgCl). To our delight, the desired product **3ea** was not observed when the reaction was performed at −0.3 V ~ −0.9 V versus Ag/AgCl. Moreover, an isolated yield of 85% can be obtained when the reaction was performed at −1.2 V versus Ag/AgCl, and the increasing voltage has practically no effect on the yield of **3ea** (Scheme 2C). The results of these potentiostatic electrolysis experiments further confirmed our speculation. Base on the aforementioned experimental results, we speculate the more reasonable mechanism of the reaction should be through the concerted PCET (vide infra) and free radical cross-coupling pathways.

Computational investigations

The density functional theory (DFT) calculation was employed to further verify our speculation on this conversion mechanism. All DFT calculations of both ground-state and transition-state structures were performed using M06-2X/6-31+G(d,p) with SMD = DMSO solvation and the Gaussian 09 software package (Frisch et al., 2009). Frequencies were calculated for all the stationary points to confirm if each optimized structure is a local minimum on the respective potential energy surface or a transition state structure with only one imaginary frequency. Scheme 3A outlines several potential reaction pathways to obtain the desired product **3ea** from 4-cyanopyridine **2a** and 4-methylquinoline **1e** under cathodic electrolysis, via sequential reduction and convergence of diradical coupling process. Reduction of each coupling partner (4-cyanopyridine and 4-methylquinoline) can occur from either its neutral entity or protonated state. For example, the subsequent radical (e.g., radical **INI2**) could add to the radical anion intermediate **1e′** (Scheme 3A, path a) or protonated state (**INT4**, Scheme 3A path b). Alternatively, the mechanism of biradical coupling (path c) could be smoothly operated, in which each coupling partner is singly reduced before a barrierless biradical coupling to afford **INT7**, which after the loss of two H^+ and one HCN would produce the desired product **3ea**. To discern between these pathways, we examined each pathway using DFT

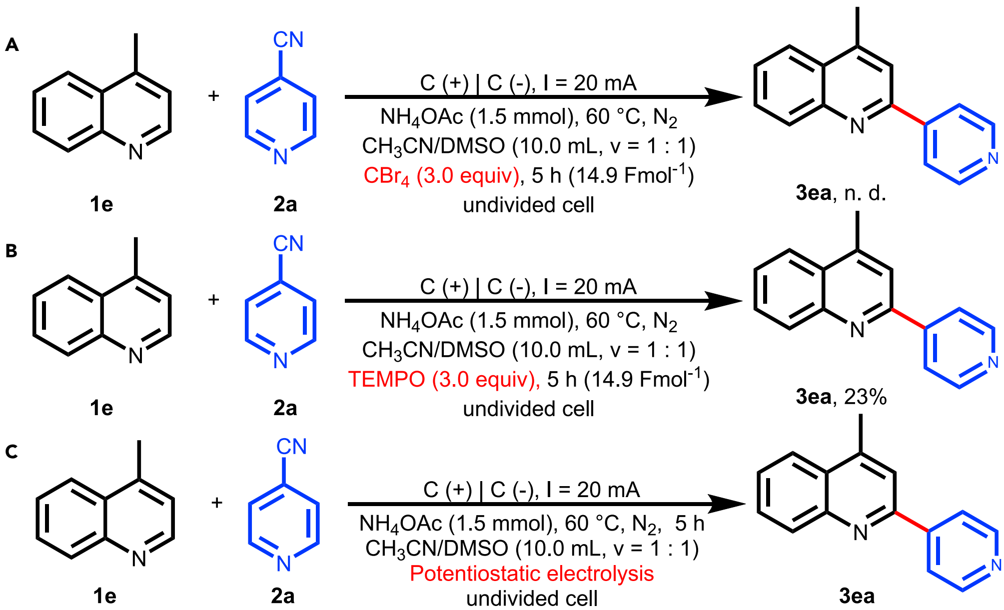

entry	Potential (V vs Ag/AgCl)	Isolated yield of **3ea** (%)
1	- 0.3 ~ - 0.9	0
2	- 1.0 for 6 h	42
3	-1.2	85
4	-1.4 for 4.5 h	86
5	-1.6 for 3.75 h	85

Scheme 2. Control experiments

calculations. The reduction of 4-methylquinoline **1e** can occur from its neutral entity or protonated state. In contrast, the electrochemical reduction of the protonated state **INT4** (E_{red} = −1.16 V versus SCE) is easier to generate the radical intermediates **INT6**. Similarly, the electroreduction of the protonated state **INT1** of 4-cyanopyridine **2a** is quite facile (E_{red} = −1.15 V versus SCE) to deliver the intermediate **INT2**, which can be demonstrated by various potentiostatic electrolysis experiments (Scheme 2C). In path a, the cross-coupling step is the reaction of radical anion intermediate **1e′** (E_{red} = - 2.06 V versus SCE) with **INT2** via transition state **TS1**, forming complex **INT3** absorbs protons to gain **INT7**. However, the determining step is that the formation of the radical anion intermediate **1e′** requires a more negative electrode potential in path a, and this conclusion can also be verified from the CV experiments of **1e** (Figure 2A). To examine path b in Scheme 3A, we performed a relaxation energy scan to afford the Minisci-type complex **INT5** between the radical intermediate **INT2** and the protonated form of **1a** by employing NH_4^+ as the acid. The energy increased monotonically without passing through a maximum as the C−C interatomic distance was decreased from 2.25 to 1.65 Å with 0.05 Å increments, suggesting this process is unfeasible. The aforementioned data suggest that path a and path b can be ruled out.

Alternatively, a biradical pathway could be invoked (Scheme 3A, path c). The intermediates **INT2** (ΔG = 3.6 kcal/mol, E_{red} = −1.15 V versus SCE) and **INT6** (ΔG = 2.7 kcal/mol, E_{red} = −1.16 V versus SCE) are simultaneously produced on the cathode surface from **2a** and **1e** with NH_4^+ via the mechanism of PCET. Subsequently, the intermediate **INT7** can be obtained through a barrierless radical cross-coupling of the intermediate **INT2** and **INT6**, with an energy release of 6.9 kcal/mol (calculated relative to the complexes [**Int2** + **INT6**]). Next, the direct dissociation of HCN molecules from **INT7** through transition state **TS2** to provide **INT8** was regarded as a routine process in the previous work. The corresponding transition state **TS3** was obtained to be 37.6 kcal/mol lower than **TS2** when the direct coordination of NH_3 to **INT7** affords **INT9** with the release of NH_4^+, suggesting the reaction pathway via **TS3** more favorable kinetically. The intermediate **INT9** removes the cyano group to give **INT10** from the transition state **TS4**, and then the

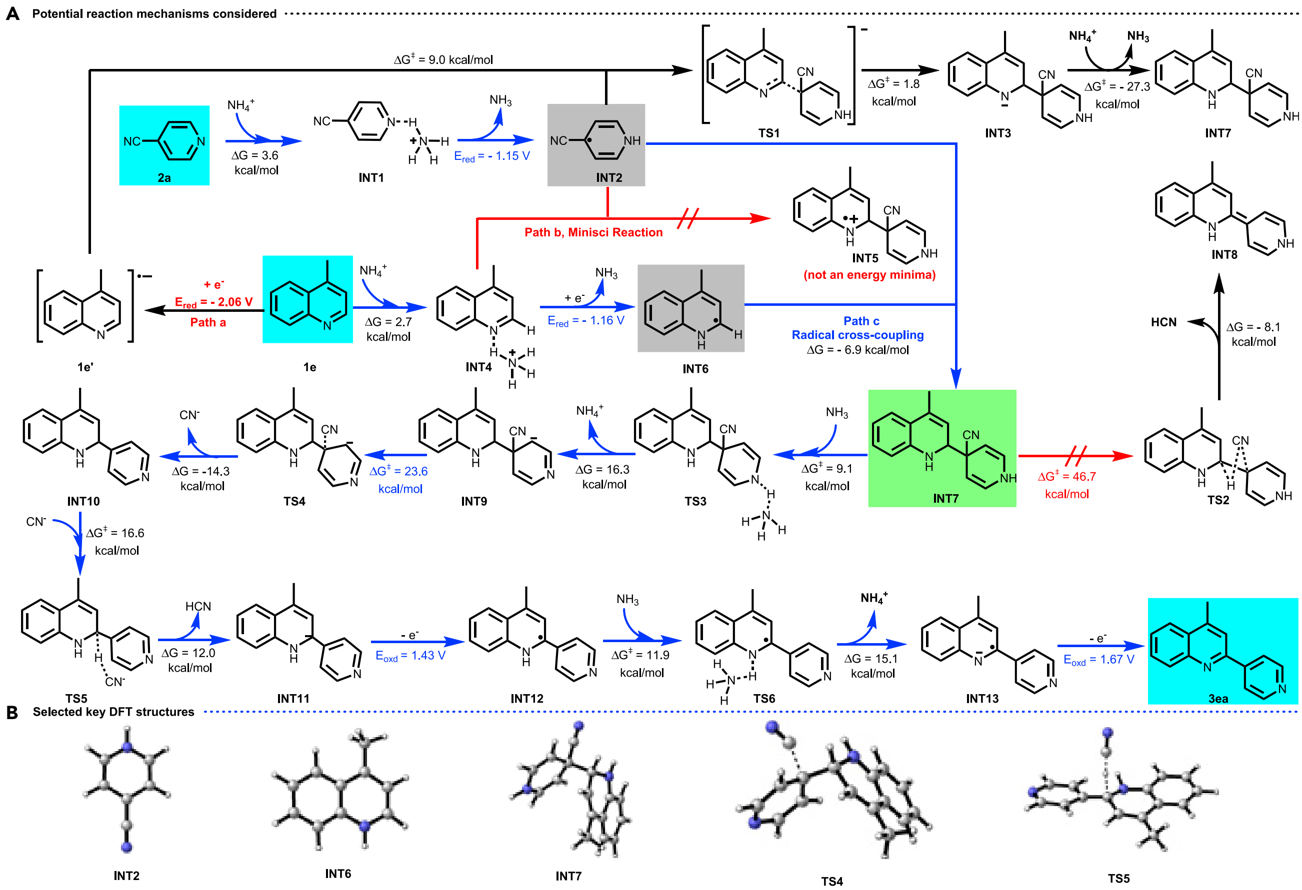

Scheme 3. Mechanistic scenarios were considered and DFT calculated data using M06-2X/6-31+G(d,p) SMD = DMSO solvation

The structures were illustrated using CYLView1 (Legault, C. Y. CYLView, 1.0b, Université de Sherbrooke, Canada, 2009, http://www.cylview.org.) Redox potentials are versus SCE. Path c is the proposed reaction pathway based on experimental and DFT data.

β-hydrogen of **INT10** is attacked by CN^- to deliver **INT11** through **TS5** with the release of HCN. Moreover, we noticed that **INT13** was obtained from **INT11** through coherent anodization and deprotonation with the help of NH_3 molecules via transition state **TS6**. Finally, the anodized intermediate **INT13** would yield the desired product **3ea**. The $\Delta G^{\ddagger}$ barrier associated with the loss of cyanide from **INT9** via rate-determining transition state **TS4** is smaller (+23.6 kcal/mol) and can be easily overcome at 60°C temperature. Furthermore, the models of key calculation intermediates have been arranged in Scheme 3B (Legault, 2009). Besides, we also checked the hydrogen generation pathways using DFT calculations and found that all pathways are infeasible starting from **INT7** and **INT10** in path c (Scheme S1).

Substrate scope

Guided by the proposed reaction mechanism, the substrate scope and limitations of the established protocol were examined under optimal reaction conditions as shown in Table 1, entry 1. Initially, the scope of the pyridylation of quinoline derivatives agreeable to this protocol was investigated based on 4-cyanopyridine **2a**. As shown in Scheme 4, a variety of quinolines bearing electron-donating and electron-withdrawing substituents in different positions are viable partners under the current protocols (**3aa-3na**) and selective, affording the corresponding products in yields of 52%–93%. Specifically, the C4 pyridylation of quinoline derivatives is the main product when C4 has no substituent. Interestingly, the desired product **4aa** can be obtained with a yield of 40% when **2a** was carried out under the given conditions, whereas only trace amounts of **3oa** and **3pa** were observed under the present protocol. Moreover, the reaction proceeded smoothly, and the corresponding products were delivered with a yield of 58%–70% when quinazoline, phenanthridine, and acridine were executed under the established conditions (**3qa-3sa**). Subsequently, the scope of the cyanopyridines was investigated by employing acridine as a

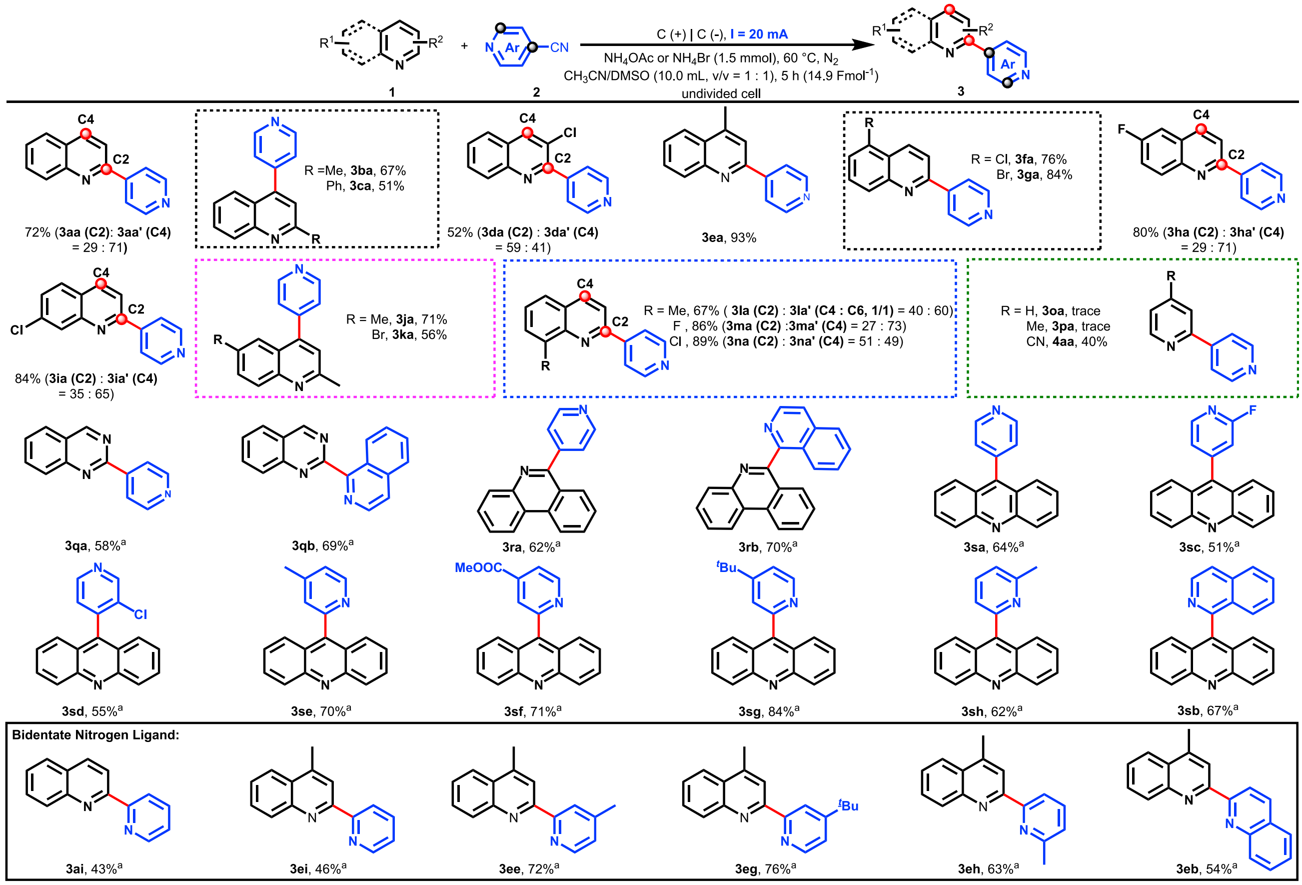

Scheme 4. Substrate scope

Reaction conditions: carbon rods (φ = 6 mm) as the anode, carbon rods (φ = 6 mm) as the cathode, constant current 20 mA, 1 (0.25 mmol), 2 (0.75 mmol), NH_4Br (1.5 mmol), CH_3CN/DMSO (1 : 1, v/v, 10.0 mL), 60 °C, N_2, 5 h (14.9 $Fmol^{-1}$). "n. d." = not detected. [a] NH_4OAc (1.5 mmol), DMSO (6.0 mL). All cited yields are isolated yields.

benchmark. To our delight, the desired products **3sc** and **3sd** can be delivered smoothly when 2-fluoroisonicotinonitrile and 3-chloroisonicotinonitrile were executed under current condition, which was difficult to achieve in previous reports (Xu et al., 2021; Zhang et al., 2020, 2021; Lehnherr et al., 2020; Wen et al., 2021). Besides, a variety of 2-cyanopyridine derivatives can also be compatible with the present protocol and deliver the corresponding products with good yields (**3se–3sb**). Unfortunately, benzonitrile and terephthalonitrile do not yield the desired product under established conditions. Finally, a series of important bidentate nitrogen ligand compounds (**3ai–3eb**) were synthesized by employing this simple and practical strategy to further enrich the types of bidentate nitrogen ligand library.

Gram-scale synthesis

The synthetic applicability of this protocol was investigated on a gram-scale reaction between **1e** or **1s** and **2a**. As shown in Scheme 5, the reaction could afford **3ea** and **3sa** in 76% and 60% yields, respectively. The results demonstrate the present protocol can serve as a simple and practical strategy to obtain the desired products via pyridylation of inert N-heterocycles.

Synthetic application

To display the potential application prospects of these compounds, **3sa** was selected as the benchmark for a series of fluorescence experiments (Figure 4) (Zou et al., 2008). At the outset, we found that **3sa** has strong fluorescence absorption in neutral and alkaline aqueous solutions (7 times stronger than acridine, Figure S84), and the obvious redshift was imagined to be caused by the acidification of **3sa** into salt in an acidic environment (Figure 4A). Subsequently, the fluorescence response of various metal ions was investigated in

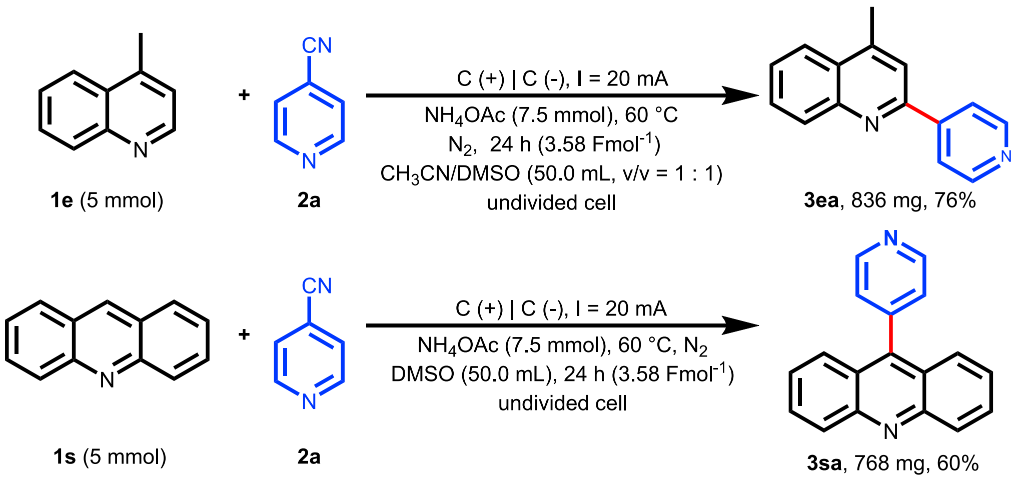

Scheme 5. Gram-scale synthesis

a neutral aqueous solution, and it was found that Fe^{2+} had a significant redshift, whereas Pd^{2+} had no absorption (Figure 4B). These results indicate that **3sa** could be served as a sensor for the fluorescence recognition of Fe^{2+} and Pd^{2+} in aqueous solutions. Moreover, the response of **3sa** for the concentration of Fe^{2+} was investigated in a neutral aqueous solution, and the results showed that the recognizable Fe^{2+} concentration was as low as 2.5×10^{-5} mmol/L (Figure 4C). Furthermore, we also found that the fluorescence redshift response concentration of Fe^{2+} ranges from 2.5×10^{-5} mmol to 2×10^{-4} mmol/L (Figure 4D).

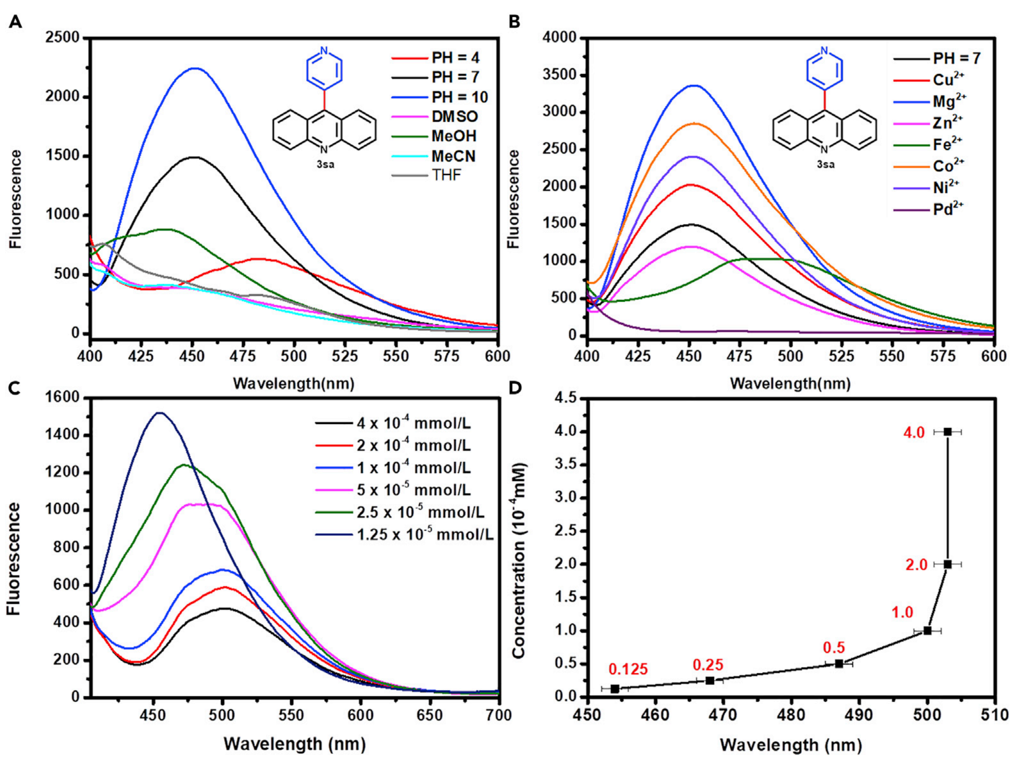

Figure 4. Fluorescence experiments

(A–C) Concentration of 3sa: 5×10^{-5} mmol/L.

(B) Concentration of metal ions: 5×10^{-5} mmol/L.

(C) Fluorescence response of different Fe^{2+} concentrations.

(D) The relationship between the concentration of Fe^{2+} and the wavelength.

Conclusion

In summary, the electrochemical NH_4^+-assisted pyridylation of the inert N-heterocycles approach has been developed. A variety of important N-fused heterocycles and bidentate nitrogen ligand compounds has been obtained via the mechanism of dual PCET and radical cross-coupling mediated by sequentially paired electrolysis. The proposed mechanism has been confirmed from experiments and DFT calculations. Moreover, the resulting product 9-(pyridin-4-yl)acridine derivatives could be served as a sensor for fluorescence recognition of Fe^{2+} and Pd^{2+}, and the recognizable Fe^{2+} concentration was as low as 2.5×10^{-5} mmol/L. Finally, we anticipate the report of this work will provide theoretical support for the activation and functionalization of N-containing compounds under electrochemical conditions.

Limitations of study

Substrate scope of inert N-heterocycles is limited to the cyanopyridine and quinoline derivatives.

STAR★METHODS

Detailed methods are provided in the online version of this paper and include the following:

- KEY RESOURCES TABLE
- RESOURCE AVAILABILITY
  - Lead contact
  - Materials availability
  - Data and code availability
- METHOD DETAILS
  - General information
  - General procedure for electrochemical ammonium cation-assisted pyridylation of inert N-heterocycles
  - Procedure for gram-scale experiments
  - Procedure for radical trapping experiments
  - Procedure for potentiostatic electrolysis
  - Cartesian coordinates of DFT optimized structures (Scheme 3)
  - Characterization data of products

SUPPLEMENTAL INFORMATION

Supplemental information can be found online at https://doi.org/10.1016/j.isci.2022.104253.

ACKNOWLEDGMENTS

This work is supported by the National Natural Science Foundation of China (No. 21902083), the Natural Science Foundation of Shandong Province (No. ZR2020QB130, ZR2021QB159). This work is also supported by the Talent Program Foundation of Qufu Normal University (NO. 6132 and 6125) and the Talent Program Foundation of Dezhou University (NO. 2021xjrc102). We acknowledge the support from Youth Innovation Team Lead-education Project of Shandong Educational Committee (NO. 301018019).

AUTHOR CONTRIBUTIONS

N. C., Y. J., and W. J. conceived the project and designed the experiments. Y. J. and W. J. wrote the manuscript. N. C., J. W., and X. J. performed and analyzed experiments. L. B. performed theoretical calculations. All the authors discussed the results of the manuscript.

DECLARATION OF INTERESTS

The authors declare no competing interests.

Received: February 11, 2022
Revised: March 15, 2022
Accepted: April 7, 2022
Published: May 20, 2022

REFERENCES

Afeli, S.A.Y., Malysz, J., and Petkov, G.V. (2013). Molecular expression and pharmacological evidence for a functional role of kv7 channel subtypes in Guinea pig urinary bladder smooth muscle. PLoS One *8*, 75875–75892. https://doi.org/10.1371/journal.pone.0075875.

Bordi, S., and Starr, J.T. (2017). Hydropyridylation of olefins by intramolecular Minisci reaction. Org. Lett. *19*, 2290–2293. https://doi.org/10.1021/acs.orglett.7b00833.

Chen, M., Zheng, X., Li, W., He, J., and Lei, A. (2010). Palladium-catalyzed aerobic oxidative cross-coupling reactions of terminal alkynes with alkylzinc reagents. J. Am. Chem. Soc. *132*, 4101–4103. https://doi.org/10.1021/ja100630p.

Chen, L. I., Chen, S., Michoud, C. (2006). Thiazolinone 3,4-disubstituted Quinolines. US20060004046 A1.

Dong, J., Yue, F., Liu, J., Song, H., Liu, Y., and Wang, Q. (2021). Visible-light-mediated three-component Minisci reaction for heteroarylethyl alcohols synthesis. Green. Chem. *23*, 7963–7968. https://doi.org/10.1039/d1gc02807c.

Felding, J., Sorensen, M.D., Poulsen, T.D., Larsen, J., Andersson, C., Refer, P., Engell, K., Ladefoged, L.G., Thormann, T., Vinggaard, A.M., et al. (2014). Discovery and early clinical development of 2-{6-[2-(3,5-dichloro-4 pyridyl)acetyl]-2,3 dimethoxy-phenoxy}-N-propylacetamide (LEO 29102), a soft-drug inhibitor of phosphodiesterase 4 for topical treatment of atopic dermatitis. J. Med. Chem. *57*, 5893–5903. https://doi.org/10.1021/jm500378a.

Frisch, M., Trucks, G., Schlegel, H., Scuseria, G., Robb, M., Cheeseman, J., Barone, V., Mennucci, B., Petersson, G., Nakatsuji, H., et al. (2009). Gaussian 09, Revision D.01 (Wallingford, CT: Gaussian, Inc.).

Gil-Martins, E., Barbosa, D.J., Silva, V., Remiao, F., and Silva, R. (2020). Dysfunction of ABC transporters at the blood-brain barrier: role in neurological disorders. Pharmacol. Ther. *213*, 107554. https://doi.org/10.1016/j.pharmthera.2020.107554.

Hey, D.H., and Williams, J.M. (1950). New therapeutic agents of the quinoline series. Part VII. 2-3-and 4-Pyridylquinolines, 4-pyridylquinaldines, and 2-pyridyllepidines. J. Chem. Soc. 1678–1683. https://doi.org/10.1039/jr9500001678.

Huang, H.-M., Bellotti, P., Ma, J., Dalton, T., and Glorius, F. (2021). Bifunctional reagents in organic synthesis. Nat. Rev. Chem. *5*, 301–321. https://doi.org/10.1038/s41570-021-00266-5.

Jin, J., and MacMillan, D.W.C. (2015). Direct α-arylation of ethers through the combination of photoredox-mediated C-H functionalization and the Minisci reaction. Angew. Chem. *127*, 1585–1589. https://doi.org/10.1002/ange.201410432.

Kim, N., Lee, C., Kim, T., and Hong, S. (2019). Visible-light-induced remote C(sp^3)–H pyridylation of sulfonamides and carboxamides. Org. Lett. *21*, 9719–9723. https://doi.org/10.1021/acs.orglett.9b03879.

Kouznetsov, V.V., Melendez Gomez, C.M., Derita, M.G., Svetaz, L., Olmo, del E., and Zacchino, S.A. (2012). Synthesis and antifungal activity of diverse C-2 pyridinyl and pyridinylvinyl substituted quinolines. Bioorg. Med. Chem. *20*, 6506–6512. https://doi.org/10.1016/j.bmc.2012.08.036.

Kouznetsov, V.V., Robles-Castellanos, M.L., Sojo, F., Rojas-Ruiz, F.A., and Arvelo, F. (2017). Diverse C-6 substituted 4-methyl-2-(2-3- and 4-pyridinyl) quinolines: synthesis, *in vitro* anticancer evaluation and in silico studies. Med. Chem. Res. *26*, 551–561. https://doi.org/10.1007/s00044-016-1775-8.

Legault, C.Y. (2009). CYLview, 1.0b (Canada: Universite de sherbrooke). http://www.cylview.org.

Lehnherr, D., Lam, Y.-H., Nicastri, M.C., Liu, J., Newman, J.A., Regalado, E.L., DiRocco, D.A., and Rovis, T. (2020). Electrochemical synthesis of hindered primary and secondary amines via proton-coupled electron transfer. J. Am. Chem. Soc. *142*, 468–478. https://doi.org/10.1021/jacs.9b10870.

Li, J.J. (2009). Minisci reaction. In Name Reactions, Jie Jack Li, ed. (Springer), pp. 361–362. https://doi.org/10.1007/978-3-030-50865-4.

Liu, Y., Yi, H., and Lei, A. (2018). Oxidation-Induced C-H functionalization: a formal way for C-H activation. J. Chem. *36*, 692–697. https://doi.org/10.1002/cjoc.201800106.

Liu, X., Liu, R., Qiu, J., Cheng, X., and Li, G. (2020). Chemical-reductant-free electrochemical deuteration reaction using deuterium oxide. Angew. Chem. Int. Ed. *59*, 13962–13967. https://doi.org/10.1002/anie.202005765.

Lu, L., Li, H., and Lei, A. (2022). Oxidative <scp>Cross-Coupling</scp> reactions between two Nucleophiles†. J. Chem. *40*, 256–266. https://doi.org/10.1002/cjoc.202100396.

Ma, X., Dang, H., Rose, J.A., Rablen, P., and Herzon, S.B. (2017). Hydroheteroarylation of unactivated alkenes using N-methoxyheteroarenium salts. J. Am. Chem. Soc. *139*, 5998–6007. https://doi.org/10.1021/jacs.7b02388.

Misale, S., Yaeger, R., Hobor, S., Scala, E., Janakiraman, M., Liska, D., Valtorta, E., Schiavo, R., Buscarino, M., Siravegna, G., et al. (2012). Emergence of KRAS mutations and acquired resistance to anti-EGFR therapy in colorectal cancer. Nature *486*, 532–536. https://doi.org/10.1038/nature11156.

Moser, S.L., Harron, S.A., Crack, J., Fawcett, J.P., and Cowley, E.A. (2008). Multiple KCNQ potassium channel subtypes mediate basal anion secretion from the human airway epithelial cell line Calu-3. J. Membr. Biol. *221*, 153–163. https://doi.org/10.1007/s00232-008-9093-9.

Murakami, K., Yamada, S., Kaneda, T., and Itami, K. (2017). C–H functionalization of azines. Chem. Rev. *117*, 9302–9332. https://doi.org/10.1021/acs.chemrev.7b00021.

Murray, P.R.D., Cox, J.H., Chiappini, N.D., Roos, C.B., McLoughlin, E.A., Hejna, B.G., Nguyen, S.T., Ripberger, H.H., Ganley, J.M., Tsui, E., et al. (2022). Photochemical and electrochemical applications of proton-coupled electron transfer in organic synthesis. Chem. Rev. *122*, 2017–2291. https://doi.org/10.1021/acs.chemrev.1c00374.

Nakao, Y. (2011). Transition-metal-catalyzed C-H functionalization for the synthesis of substituted pyridines. Synthesis *2011*, 3209–3219. https://doi.org/10.1055/s-0030-1260212.

Novaes, L.F.T., Liu, J., Shen, Y., Lu, L., Meinhardt, J.M., and Lin, S. (2021). Electrocatalysis as an enabling technology for organic synthesis. Chem. Soc. Rev. *50*, 7941–8002. https://doi.org/10.1039/d1cs00223f.

Nunn, A.J., and Schofield, K. (1952). Some o-aminophenyl-pyridyl- and -quinolyl-carbinols. J. Chem. Soc. 589–594. https://doi.org/10.1039/jr9520000589.

Pang, X., Wu, M., Ni, J., Zhang, F., Lan, J., Chen, B., and Yan, R. (2017). Copper-catalyzed tandem aerobic oxidative cyclization for the synthesis of polysubstituted quinolines via C(sp^3)/C(sp^2)–H bond functionalization. J. Org. Chem. *82*, 10110–10120. https://doi.org/10.1021/acs.joc.7b01575.

Peters, B.K., Rodriguez, K.X., Reisberg, S.H., Beil, S.B., Hickey, D.P., Kawamata, Y., Collins, M., Starr, J., Chen, L., Klunder, K., et al. (2019). Scalable and safe synthetic organic electroreduction inspired by Li-ion battery chemistry. Science *363*, 838–845. https://doi.org/10.1126/science.aav5606.

Proctor, R.S.J., and Phipps, R.J. (2019). Recent advances in Minisci-type reactions. Angew. Chem. Int. Ed. *58*, 13666–13699. https://doi.org/10.1002/anie.201900977.

Roder, L., Nicholls, A.J., and Baxendale, I.R. (2019). Flow hydrodediazoniation of aromatic heterocycles. Molecules *24*, 1996–2014. https://doi.org/10.3390/molecules24101996.

Shen, J., Zhang, Y., Yu, Y., and Wang, M. (2021). Metal-free visible-light-induced photoredox-catalyzed intermolecular pyridylation/phosphinoylation of alkenes. Org. Chem. Front. *8*, 901–907. https://doi.org/10.1039/d0qo01218a.

Tay, N.E.S., Lehnherr, D., and Rovis, T. (2022). Photons or electrons? a critical comparison of electrochemistry and photoredox catalysis for organic synthesis. Chem. Rev. *122*, 2487–2649. https://doi.org/10.1021/acs.chemrev.1c00384.

Tong, S., Li, K., Ouyang, X., Song, R., and Li, J. (2021). Recent advances in the radical-mediated decyanative alkylation of cyano (hetero) arene. Green. Synth. Catal. *2*, 145–155. https://doi.org/10.1016/j.gresc.2021.04.003.

Wang, Q.-Q., Xu, K., Jiang, Y.-Y., Liu, Y.-G., Sun, B.-G., and Zeng, C.-C. (2017). Electrocatalytic Minisci acylation reaction of N-heteroarenes mediated by NH_4I. Org. Lett. *19*, 5517–5520. https://doi.org/10.1021/acs.orglett.7b02589.

Wang, D., Désaubry, L., Li, G., Huang, M., and Zheng, S. (2021). Recent advances in the synthesis of C2-functionalized pyridines and quinolines using N-oxide chemistry. Adv. Synth. Catal. *363*, 2–39. https://doi.org/10.1002/adsc.202000910.

Wen, J., Yang, X., Yan, K., Qin, H., Ma, J., Sun, X., Yang, J., and Wang, H. (2021). Electroreductive

C3 pyridylation of quinoxalin-2 (1 H)-ones: an effective way to access bidentate nitrogen ligands. Org. Lett. *23*, 1081–1085. https://doi.org/10.1021/acs.orglett.0c04296.

Wu, Y., Zeng, L., Li, H., Cao, Y., Hu, J., Xu, M., Shi, R., Yi, H., and Lei, A. (2021). Electrochemical palladium-catalyzed oxidative sonogashira carbonylation of arylhydrazines and alkynes to ynones. J. Am. Chem. Soc. *143*, 12460–12466. https://doi.org/10.1021/jacs.1c06036.

Xu, H., Liu, J., Nie, F., Zhao, X., and Jiang, Z. (2021). Metal-free hydropyridylation of thioester-activated alkenes via electroreductive radical coupling. J. Org. Chem. *86*, 16204–16212. https://doi.org/10.1021/acs.joc.1c01526.

Yadav, J.S., and Reddy, B.V.S. (2003). Microwave-assisted rapid synthesis of neurotransmitter release enhancer linopiridine and its new analogues. Synth. Commun. *33*, 3115–3121. https://doi.org/10.1081/scc-120023425.

Yamaguchi, T., Sakairi, K., Yamaguchi, E., Tada, N., and Itoh, A. (2016). Magnesium iodide-catalyzed synthesis of 2-substituted quinazolines using molecular oxygen and visible light. RSC Adv. *6*, 56892–56895. https://doi.org/10.1039/C6RA04073J.

Yang, J., Ma, J., Yan, K., Tian, L., Li, B., and Wen, J. (2022). Electrochemical ammonium cation-assisted hydropyridylation of ketone-activated alkenes: experimental and computational mechanistic studies. Adv. Synth. Catal. *364*, 845–854. https://doi.org/10.1002/adsc.202101361.

Yuan, Y., Qi, J.C., Qi, J., Wang, D.X., Wang, D., Chen, Z., Wan, H., Zhu, J., Yi, H., Chowdhury, A.D., and Lei, A. (2021). Radical–radical cross-coupling assisted N–S bond formation using alternating current protocol. CCS Chem. *3*, 3027–3038. https://doi.org/10.31635/ccschem.021.202101350.

Zhang, X., Yang, C., Gao, H., Wang, L., Guo, L., and Xia, W. (2021). Reductive arylation of aliphatic and aromatic aldehydes with cyanoarenes by electrolysis for the synthesis of alcohols. Org. Lett. *23*, 3472–3476. https://doi.org/10.1021/acs.orglett.1c00920.

Zhang, Y., Geng, Z., Li, J., Zou, D., Wu, Y., and Wu, Y. (2017a). Ligand-controlled palladium-catalyzed pyridylation of 1-*tert*-butoxycarbonyl-3-iodoazetidine: regioselective synthesis of 2-and 3-heteroarylazetidines. Adv. Synth. Catal. *359*, 390–394. https://doi.org/10.1002/adsc.201600470.

Zhang, G., Wu, J., Zeng, H., Zhang, S., Yin, Z., and Zheng, S. (2017b). Cobalt-catalyzed α-alkylation of ketones with primary alcohols. Org. Lett. *19*, 1080–1083. https://doi.org/10.1021/acs.orglett.7b00106.

Zhang, S., Li, L., Li, X., Zhang, J., Xu, K., Li, G., and Findlater, M. (2020). Electroreductive 4-Pyridylation of electron-deficient alkenes with assistance of $Ni(acac)_2$. Org. Lett. *22*, 3570–3575. https://doi.org/10.1021/acs.orglett.0c01014.

Zeng, L., Li, H., Hu, J., Zhang, D., Hu, J., Peng, P., Wang, S., Shi, R., Peng, J., Pao, C.-W., et al. (2020). Electrochemical oxidative aminocarbonylation of terminal alkynes. Nat. Catal. *3*, 438–445. https://doi.org/10.1038/s41929-020-0443-z.

Zhao, Y., Wang, H., Hou, X., Hu, Y., Lei, A., Zhang, H., and Zhu, L. (2006). Oxidative cross-coupling through double transmetallation: surprisingly high selectivity for palladium-catalyzed cross-coupling of alkylzinc and alkynylstannanes. J. Am. Chem. Soc. *128*, 15048–15049. https://doi.org/10.1021/ja0647351.

Zhou, F.-Y., and Jiao, L. (2021). Recent developments in transition-metal-free functionalization and derivatization reactions of pyridines. Synlett *32*, 159–178. https://doi.org/10.1055/s-0040-1706552.

Zhu, S., Qin, J., Wang, F., Li, H., and Chu, L. (2019). Photoredox-catalyzed branch-selective pyridylation of alkenes for the expedient synthesis of Triprolidine. Nat. Commun *10*, 749–756. https://doi.org/10.1038/s41467-019-08669-1.

Zou, Y., Young, D.D., Cruz-Montanez, A., and Deiters, A. (2008). Synthesis of anthracene and azaanthracene fluorophores via [2+2+2] cyclotrimerization reactions. Org. Lett. *10*, 4661–4664. https://doi.org/10.1021/ol8019549.

STAR★METHODS

KEY RESOURCES TABLE

REAGENT or RESOURCE	SOURCE	IDENTIFIER
Chemicals, peptides, and recombinant proteins		
Quinoline	Adamas	91-22-5
2-Methylquinoline	Adamas	91-63-4
2-Phenylquinoline	Aladdin	612-96-4
3-Chloroquinoline	Arkpharm	612-59-9
4-Methylquinoline	Adamas	491-35-0
5-Chloroquinoline	Aladdin	635-27-8
5-Bromoquinoline	Adamas	4964-71-0
6-Fluoroquinoline	Adamas	396-30-5
7-Chloroquinoline	Aladdin	612-61-3
2,6-Dimethylquinoline	Macklin	877-43-0
6-Bromo-2-methylquinoline	Macklin	877-42-9
8-Methylquinoline	Adamas	611-32-5
8-Fluoroquinoline	Adamas	394-68-3
8-Chloroquinoline	Aladdin	611-33-6
Pyridine	Adamas	110-86-1
4-Methylpyridine	Adamas	108-89-4
Quinazoline	Arkpharm	253-82-7
Phenanthridine	MREDA	229-87-8
Acridine	Macklin	260-94-6
4-Cyanopyridine	Macklin	100-48-1
Isoquinoline-1-carbonitrile	Macklin	1198-30-7
2-Fluoroisonicotinonitrile	Macklin	3939-14-8
3-Chloro-4-cyanopyridine	Aladdin	68325-15-5
4-Methyl-2-pyridinecarbonitrile	Adamas	1620-76-4
Methyl 2-cyanoisonicotinate	Arkpharm	94413-64-6
4-tert-butylpyridine-2-carbonitrile	Bidei	42205-73-2
2-Cyano-6-methylpyridine	Aladdin	1620-75-3
NH_4OAc	Adamas	631-61-8
NH_4Br	Aladdin	12124-97-9
NH_4I	Adamas	12027-06-4

RESOURCE AVAILABILITY

Lead contact

Further information and requests for resources should be directed to and will be fulfilled by the lead contact, Jiangwei Wen (wenjy@qfnu.edu.cn).

Materials availability

All materials generated in this study are available in the article and supplemental information or from the lead contact without restriction upon reasonable request.

Data and code availability

Any additional information required to reanalyze the data reported in this paper is available from the lead contact upon request.

METHOD DETAILS

General information

All glassware was oven dried at 100°C for hours and cooled down under vacuum. Unless otherwise noted, materials were obtained from commercial suppliers and used without further purification. The instrument for electrolysis is dual display potentiostat (DJS-292B) (made in China), the carbon rod (d: 6 mm) was purchased from Xuzhou Xinke Instrument and Meter Co. LTD. Cyclic voltammetry was performed in a three-necked flask (25.0 mL) with CHI760E as the electrochemical workstation, glassy carbon as the working electrode, Pt ($1.5 \times 1.5\ cm^{-1}$) as the counter electrode, and Ag/AgCl (KCl) as the reference electrode. Thin-layer chromatography (TLC) employed glass 0.25 mm silica gel plates. Flash chromatography columns were packed with 200–300 mesh silica gel in petroleum (b. p. 60-90°C). ^{1}H, ^{13}C NMR, and ^{19}F NMR data were recorded with Bruker Advance III (500 MHz) spectrometers with tetramethylsilane as an internal standard. All chemical shifts (δ) are reported in ppm and coupling constants (J) in Hz. All chemical shifts are reported relative to tetramethylsilane and d-solvent peaks (77.00 ppm, chloroform), respectively.

General procedure for electrochemical ammonium cation-assisted pyridylation of inert N-heterocycles

In an oven-dried undivided three-necked flask (25 mL) equipped with a stir bar, **1** (0.25 mmol), **2** (0.75 mmol), and NH_4OAc (1.5 mmol, 115.5 mg) or NH_4Br (1.5 mmol, 145.5 mg) were combined and added. The flask was equipped with carbon rods (φ = 6 mm) as the anode and carbon rods (φ = 6 mm) as the cathode (distance between electrodes (5 - 10 mm)) and was then charged with nitrogen. Under the protection of nitrogen, DMSO (6.0 mL) or DMSO/CH_3CN (10.0 mL, v/v = 1 : 1) were slowly injected into the reaction flask. The reaction mixture was stirred and electrolyzed at a constant current of 20 mA under 60°C for 5 h. When the reaction was finished, the reaction mixture was washed with water and extracted with CH_2Cl_2 (10 mL x 3). The organic layers were combined, dried over Na_2SO_4, and concentrated. The pure product was obtained by flash column chromatography on silica gel (Scheme 4).

Procedure for gram-scale experiments

In an oven-dried undivided three-necked flask (150 mL) equipped with a stir bar, **1e** or **1s** (5.0 mmol), **2a** (35.0 mmol), and NH_4OAc (7.5 mmol, 577.5 mg) were combined and added. The flask was equipped with carbon rods (φ = 6 mm) as the anode and carbon rods (φ = 6 mm) as the cathode and was then charged with nitrogen. Under the protection of nitrogen, DMSO (50.0 mL) or CH_3CN/DMSO (50.0 mL, v = 1/1) was slowly injected into the reaction flask. The reaction mixture was stirred and electrolyzed at a constant current of 20 mA under 60°C for 24 h (3.58 $Fmol^{-1}$). When the reaction was finished, the reaction mixture was washed with water and extracted with CH_2Cl_2 (10 mL x 3). The organic layers were combined, dried over Na_2SO_4, and concentrated. The pure products **3ea** and **3sa** were obtained with isolated yields of 76 and 60%, respectively (Scheme 5).

Procedure for radical trapping experiments

In an oven-dried undivided three-necked flask (25 mL) equipped with a stir bar, **2a** (0.75 mmol, 78.0 mg), CBr_4 or TEMPO (0.75 mmol), and NH_4OAc (1.5 mmol, 115.5 mg) were combined and added. The flask was equipped with a carbon rods (φ = 6 mm) as the anode and carbon rods (φ = 6 mm) as the cathode and was then charged with nitrogen. Under the protection of nitrogen, CH_3CN (5.0 mL), DMSO (5.0 mL), and **1e** (0.25 mmol, 33.0 μL) were slowly injected into the reaction flask. The reaction mixture was stirred and electrolyzed at a constant current of 20 mA under 60°C for 5 h (14.9 $Fmol^{-1}$). After the reaction was completed, the solution was concentrated in a vacuum and not detected the desired product **3ea** when CBr_4 was added. Only 24% yield of the product can be obtained when TEMPO was added into the reaction (Schemes 2A and 2B).

Procedure for potentiostatic electrolysis

In an oven-dried undivided three-necked flask (25 mL) equipped with a stir bar, **1e** (0.25 mmol), **2a** (0.75 mmol), and NH_4OAc (1.5 mmol, 115.5 mg) were combined and added. The flask was equipped with carbon rods (φ = 6 mm) as the anode and carbon rods (φ = 6 mm) as the cathode and was then charged with nitrogen. Under the protection of nitrogen, CH_3CN/DMSO (10.0 mL, v = 1/1) was slowly injected into the reaction flask. The reaction mixture was stirred and potentiostatic electrolysis under 60°C. When the reaction was finished, the reaction mixture was washed with water and extracted with CH_2Cl_2 (10 mL x 3). The organic layers were combined, dried over Na_2SO_4, and concentrated. The pure products **3ea** was obtained with isolated yields of 42–86%, respectively (Scheme 2C).

Cartesian coordinates of DFT optimized structures (Scheme 3)

Structure: **2a**

Charge = 0 Multiplicity = 1

Number of imaginary frequencies: 0

SCF Energy: -340.405766087 hartree

SCF Energy + ZPVE: -340.317523087 hartree

Free Energy: -340.347767 hartree

C	-2.571884265	1.008116473 0	000077007
C	-1.175925754 1	010471325 0	000502393
C	-0.533527459	2.245577093	0.000136667
C	-2.519576754	3.392171115	0.001469848
C	-3.267667316	2.218197647	0.000937630
H	-0.609408387	0.086322260	0.001278108
H	0.551840938	2.292079008	0.000171440
H	-3.022314843	4.355143705	0.002257963
H	-4.351332571	2.246710177	0.001289817
C	-3.293429947	0.240181311	0.000662913
N	-3.871729476	1.242053748	0.001118242
N	-1.182578166	3.414798258	0.001092178

Structure: NH_4^+

Charge = 1 Multiplicity = 1

Number of imaginary frequencies: 0

SCF Energy: -56.997554118 hartree

SCF Energy + ZPVE: -56.948082118 hartree

Free Energy: -56.967730 hartree

N	-3.902376867	-1.296316683	0.000861666
H	-3.106389072	-0.750596627	0.341988950
H	-3.828533098	-2.258260512	0.342612795
H	-4.772431434	-0.878589496	0.342376399
H	-3.902166819	-1.296676883	-1.022342560

Structure: **INT1**

Charge = 1 Multiplicity = 1

Number of imaginary frequencies: 0

SCF Energy: -397.412869783 hartree

SCF Energy + ZPVE: -397.273779783 hartree

Free Energy: -397.309668 hartree

C	-2.632155052	0.905361098	0.000711693
C	-1.236971127	0.878148354	-0.038639565
C	-0.567743188	2.097210065	-0.036037398
C	-2.542062020	3.286756245	0.039368787
C	-3.307638473	2.126260559	0.040957691
H	-0.690582873	-0.057240871	-0.069647369
H	0.517169651	2.131976685	-0.065404396
H	-3.017961154	4.262534336	0.068613668
H	-4.389916041	2.173133325	0.071975577
C	-3.378123927	-0.328983753	-0.000377612
N	-3.976194282	-1.318784634	-0.001232607
N	-1.205609600	3.271782849	0.001750035
H	-0.364255870	4.795286580	-0.004040776
N	0.120127860	5.742962879	-0.005624028
H	0.071744158	6.159739574	-0.937825039
H	-0.333933779	6.369661685	0.662237495
H	1.102045717	5.634750025	0.257823845

Structure: NH_3

Charge = 0 Multiplicity = 1

Number of imaginary frequencies: 0

SCF Energy: -56.535103739 hartree

SCF Energy + ZPVE: -56.500700739 hartree

Free Energy: -56.519774 hartree

N	-3.874864593	-1.277270739	0.012925493
H	-3.839302820	-2.242233063	0.330833468
H	-4.761760890	-0.894673414	0.330235737
H	-3.911584047	-1.302886074	-1.002678548

Structure: INT2

Charge = 0 Multiplicity = 2

Number of imaginary frequencies: 0

SCF Energy: -340.984355474 hartree

SCF Energy + ZPVE: -340.885420474 hartree

Free Energy: -340.916771 hartree

C	-2.625614870	0.915486388	0.000117019
C	-1.190496524	0.944926376	0.000538036
C	-0.534952869	2.136576333	-0.000067998
C	-2.613074753	3.336464230	-0.001493200
C	-3.317554432	2.173163608	-0.000928158
H	-0.619407753	0.023642152	0.001334928
H	0.544290599	2.220436237	0.000207966
H	-3.079964374	4.313115715	-0.002257037
H	-4.400993132	2.207334391	-0.001258608
C	-3.328365783	-0.301726503	0.000703575
N	-3.913051903	-1.314732364	0.001188513
N	-1.235910945	3.322170170	-0.001084947
H	-0.730234263	4.199111267	-0.001537088

Structure: **1e**

Charge = 0 Multiplicity = 1

Number of imaginary frequencies: 0

SCF Energy: -441.084039483 hartree

SCF Energy + ZPVE: -440.919256483 hartree

Free Energy: -440.952206 hartree

C	-6.052787032	0.198268067	0.004442261
C	-4.679378011	0.234322053	0.004240657
C	-3.990412913	1.476567647	0.004374773
C	-4.737154211	2.688138076	0.004709541
C	-6.156801963	2.618571489	0.004903976
C	-6.799192167	1.402753683	0.004776347
H	-6.572388904	-0.755121859	0.004343742
H	-4.088670151	-0.677337313	0.003985549
C	-4.021330757	3.927505617	0.004833892
H	-6.735463755	3.537122220	0.005155339
H	-7.884123641	1.361810148	0.004928006
C	-2.647808027	3.864453918	0.004622763
C	-1.996526890	2.606650612	0.004296614
H	-2.050857765	4.771412918	0.004702891
H	-0.908567346	2.572214846	0.004118963
N	-2.622393020	1.451477026	0.004162886
C	-4.748731360	5.240331314	0.005182644
H	-5.391314758	5.331814259	-0.876784405
H	-5.391057754	5.331490908	0.887370542
H	-4.040104575	6.070889372	0.005232019

Structure: **1e′**

Charge = -1 Multiplicity = 2

Number of imaginary frequencies: 0

SCF Energy: -441.158308434 hartree

SCF Energy + ZPVE: -440.998059434 hartree

Free Energy: -441.031990 hartree

C	-6.087369789	0.195105912	0.004457004
C	-4.682835599	0.237470034	0.004269133
C	-3.976751039	1.461728019	0.004382576
C	-4.736528928	2.694326508	0.004696802
C	-6.152439852	2.615676993	0.004881879
C	-6.818879512	1.378634621	0.004755561
H	-6.598048742	-0.764711389	0.004348504
H	-4.101619629	-0.681741731	0.004029013
C	-4.019799349	3.926615093	0.004819292
H	-6.732363245	3.534413117	0.005119557
H	-7.905712968	1.351889271	0.004891948
C	-2.609564466	3.861909219	0.004582019
C	-1.967370859	2.635804527	0.004283273
H	-2.021305247	4.777180741	0.004651253
H	-0.878984037	2.591305885	0.004111179
N	-2.608250485	1.439639750	0.004184028
C	-4.753895299	5.234925909	0.005204020
H	-5.405762658	5.344600745	-0.874084158
H	-5.405479494	5.344230311	0.884748441
H	-4.052104801	6.074331464	0.005270675

Structure: **TS1**

Charge = -1 Multiplicity = 1

Number of imaginary frequencies: 1

SCF Energy: -782.156567594 hartree

SCF Energy + ZPVE: -781.894427594 hartree

Free Energy: -781.934341 hartree

C	-2.322445394	7.635236839	1.511953960
C	-3.188124982	6.656092180	1.060110682
C	-2.709140329	5.439986945	0.494140779
C	-1.288557537	5.254956055	0.443442355
C	-0.432573653	6.266462959	0.913087281
C	-0.928755279	7.453640971	1.437445988
H	-2.725173584	8.555977635	1.926852984

H	-4.264673131	6.799913279	1.115088049
C	-0.803358098	3.984985820	-0.069446134
H	0.642869496	6.114503813	0.861924304
H	-0.252229318	8.226285170	1.789180131
C	-1.714833778	3.089401033	-0.525283140
C	-3.128162811	3.425297612	-0.597309245
H	-1.388797334	2.124381142	-0.905670957
N	-3.607163741	4.511173367	0.075386782
C	0.670297113	3.687348540	-0.091526135
H	1.116821171	3.768301860	0.905774205
H	0.851644617	2.678599660	-0.471131045
H	1.200387167	4.395359921	-0.740415291
C	-3.319730153	3.740144001	-2.675829815
C	-2.882759428	2.501391115	-3.366123034
C	-1.635919502	2.386731110	-3.856215998
C	-1.207849424	4.709630570	-3.476205108
C	-2.446060627	4.894908248	-2.984768140
H	-3.563615813	1.659140078	-3.442474236
H	-1.274045458	1.480081899	-4.328524879
H	-0.523805602	5.530660007	-3.661554115
H	-2.785458502	5.902555392	-2.764409212
N	-0.705944135	3.431924624	-3.768676101
H	-3.819489283	2.582058002	-0.654850610
C	-4.716963353	3.982227683	-2.670174461
N	-5.867752626	4.148334663	-2.542310816
H	0.067010313	3.395747806	-4.420387031

Structure: INT3

Charge = -1 Multiplicity = 1

Number of imaginary frequencies: 0

SCF Energy: -782.166007206 hartree

SCF Energy + ZPVE: -781.901971206 hartree

Free Energy: -781.945969 hartree

C	-2.276059373	7.692487922	1.552609220
C	-3.133694011	6.693678891	1.128328866
C	-2.655538424	5.452439212	0.588291952
C	-1.218808081	5.283291431	0.584183724
C	-0.380749837	6.313022251	1.028558166
C	-0.879437516	7.527731010	1.498897100
H	-2.694374984	8.622352005	1.933123935
H	-4.211146872	6.839605161	1.174786637
C	-0.716627444	3.961619870	0.208956061
H	0.696085022	6.156254601	1.009150144
H	-0.209647977	8.316179549	1.826824900

C	-1.584233352	3.050529624	-0.274760490
C	-3.021276622	3.395350738	-0.556088950
H	-1.244038091	2.040590927	-0.497434618
N	-3.533176041	4.533786913	0.171575179
C	0.736986643	3.629427418	0.421050107
H	1.037019965	3.782532600	1.463915522
H	0.938135828	2.589400491	0.150723108
H	1.380138000	4.269760607	-0.194281009
C	-3.220079639	3.602700093	-2.134908458
C	-2.822737583	2.364060097	-2.916152821
C	-1.743088971	2.337537184	-3.714548928
C	-1.387815029	4.676870958	-3.458271487
C	-2.452528326	4.803714041	-2.650079880
H	-3.404540280	1.458891112	-2.773180766
H	-1.430709654	1.436221406	-4.230974212
H	-0.807020070	5.533221488	-3.783644401
H	-2.749049154	5.789022270	-2.306869646
N	-0.955691445	3.451191301	-3.932618783
H	-3.648518007	2.514109595	-0.340608798
C	-4.669051682	3.834763489	-2.329509635
N	-5.806791217	3.982385568	-2.493771101
H	-0.242454119	3.420549361	-4.646486599

Structure: INT7

Charge = 0 Multiplicity = 1

Number of imaginary frequencies: 0

SCF Energy: -782.675159941 hartree

SCF Energy + ZPVE: -782.396750941 hartree

Free Energy: -782.440196 hartree

C	-5.774017340	-0.058304785	0.537500326
C	-4.435234650	0.211257689	0.806215340
C	-3.899434824	1.476626908	0.524818251
C	-4.729457589	2.484776826	-0.020616722
C	-6.071565308	2.187207826	-0.278995825
C	-6.600842618	0.924948452	-0.011214088
H	-6.171572997	-1.045485171	0.755780082
H	-3.790078067	-0.553499489	1.231391387
C	-4.139528624	3.813839388	-0.254661762
H	-6.713499033	2.957362903	-0.697084093
H	-7.643562517	0.712922931	-0.224170484
C	-2.810940089	3.979165640	-0.134632617
C	-1.873537462	2.842641496	0.162982682
H	-2.365237290	4.956425563	-0.297866199
H	-1.068707799	3.188864695	0.823036297

N	-2.587466241	1.776930054	0.835464553
C	-5.045428673	4.956706372	-0.620463731
H	-5.544198580	4.766662909	-1.577829284
H	-5.830226674	5.098560038	0.130528898
H	-4.475566575	5.884354588	-0.710515772
H	-2.025231898	1.005248656	1.176709163
C	-1.150150995	2.358390933	-1.172647823
C	-0.344626973	3.491283074	-1.780941038
C	-0.747514416	4.117051195	-2.898878053
C	-2.454820597	2.510838972	-3.295165170
C	-2.128002158	1.812894804	-2.195403514
H	0.541496203	3.834065855	-1.257639557
H	-0.212268714	4.967741584	-3.306242045
H	-3.196869236	2.155907777	-4.001956560
H	-2.607739459	0.859874402	-2.000179827
C	-0.229453154	1.273357674	-0.762248221
N	0.479144553	0.425287723	-0.416920526
N	-1.861482261	3.718189553	-3.609377111
H	-2.041514948	4.133699965	-4.512287954

Structure: INT4

Charge = -1 Multiplicity = 1

Number of imaginary frequencies: 1

SCF Energy: -782.163198498 hartree

SCF Energy + ZPVE: -781.900079498 hartree

Free Energy: -781.943687 hartree

C	-5.831076442	-0.074705223	0.502742400
C	-4.475706458	0.187351210	0.679949856
C	-3.972652842	1.483068775	0.486056441
C	-4.853966523	2.525426051	0.111934318
C	-6.212057530	2.235205983	-0.056394348
C	-6.709597498	0.945780466	0.130972133
H	-6.201053016	-1.085000491	0.653554042
H	-3.791671994	-0.606874088	0.968607070
C	-4.292584786	3.877132925	-0.055269156
H	-6.891756696	3.033199130	-0.341548141
H	-7.765937220	0.741071698	-0.009987457
C	-2.960091880	4.045557961	-0.032308380
C	-1.979520858	2.910129881	0.117885117
H	-2.534974215	5.037418639	-0.165032026
H	-1.169922458	3.225667064	0.787654109
N	-2.642192444	1.766927632	0.723140631
C	-5.231797300	5.034737367	-0.253418793

H	-5.812300986	4.915734167	-1.175304088
H	-5.948184626	5.109627017	0.572173696
H	-4.675971841	5.972983556	-0.318534979
H	-2.043720215	0.959296002	0.862044759
C	-1.312489842	2.590535999	-1.242109956
C	-0.488189104	3.652306021	-1.801221591
C	-0.271410741	3.725599036	-3.156228309
C	-1.825426561	2.128800732	-3.597943117
C	-2.131729012	1.962000174	-2.268272924
H	0.040623967	4.324062321	-1.128926955
H	0.421743641	4.475699862	-3.537764074
H	-2.400164592	1.575764638	-4.341271285
H	-2.916570840	1.267601849	-1.980446261
C	-0.119416787	1.284269494	-0.685446641
N	0.759718706	0.521459055	-0.793269689
N	-0.877031008	2.958730097	-4.093226403

Structure: INT6

Charge = 0 Multiplicity = 2

Number of imaginary frequencies: 0

SCF Energy: -441.652756029 hartree

SCF Energy + ZPVE: -441.478331029 hartree

Free Energy: -441.512412 hartree

C	-6.078091951	0.217142851	-0.047374163
C	-4.680837321	0.264851071	-0.010146191
C	-4.021818173	1.495050747	0.010785480
C	-4.751314099	2.722186199	-0.005244947
C	-6.159342481	2.634445728	-0.042733249
C	-6.813673066	1.401564168	-0.062990418
H	-6.581840817	-0.744357616	-0.063492697
H	-4.092764064	-0.649168533	0.002279034
C	-4.035762644	3.969809855	0.016790608
H	-6.742850700	3.549826771	-0.055657208
H	-7.898802210	1.369364249	-0.091397154
C	-2.626636632	3.927330151	0.054732606
C	-1.942287084	2.737958116	0.069508736
H	-2.058193272	4.852470672	0.072215424
H	-0.863566274	2.658847575	0.097773947
N	-2.638657000	1.549848038	0.047957838
C	-4.782170921	5.268998673	0.000282489
H	-5.408876380	5.369392855	-0.896377456
H	-5.454353043	5.365944423	0.863812353
H	-4.086897379	6.112291530	0.019877913
H	-2.125345490	0.677068477	0.058419055

Structure: TS2

Charge = 0 Multiplicity = 1

Number of imaginary frequencies: 1

SCF Energy: -782.583335878 hartree

SCF Energy + ZPVE: -782.311381878 hartree

Free Energy: -782.354800 hartree

C	-6.108954945	-0.239240507	-0.191950784
C	-4.818412379	-0.154034572	-0.686809032
C	-4.068235170	1.004758267	-0.445778593
C	-4.603664813	2.087468882	0.279746934
C	-5.917913725	1.970950319	0.769508482
C	-6.660673808	0.823587799	0.540688852
H	-6.693410666	-1.136030116	-0.372971224
H	-4.375766687	-0.968112052	-1.254108563
C	-3.778035312	3.271586058	0.466816523
H	-6.351873192	2.791234745	1.332525865
H	-7.671885675	0.747449111	0.927245097
C	-2.498152873	3.259405239	0.010340437
C	-1.931627352	2.107860979	-0.644557922
H	-1.848520752	4.118229121	0.158632425
H	-0.649600897	1.829805342	0.475663322
N	-2.780383455	1.110446596	-0.944240489
C	-4.347060990	4.471278903	1.163684300
H	-5.249064430	4.826254541	0.654309533
H	-4.628962619	4.224464595	2.193233713
H	-3.616872697	5.282246205	1.190135850
H	-2.424055160	0.337821255	-1.506559050
C	-0.654803956	2.248645448	-1.526428167
C	-0.791692065	3.297980956	-2.596518160
C	-0.755324744	3.003249358	-3.910351214
C	-0.225665512	0.730716252	-3.470699281
C	-0.256069466	0.928436137	-2.139239915
H	-0.950794570	4.326854970	-2.289206946
H	-0.889911732	3.757975420	-4.677661331
H	0.054463241	-0.223298718	-3.904191497
H	0.017985121	0.114530702	-1.472954043
C	0.288550963	2.541800808	-0.367695681
N	1.294974207	3.084742973	-0.020269914
N	-0.527128775	1.727086822	-4.368210891
H	-0.444336673	1.553119139	-5.359619202

Structure: INT8

Charge = 0 Multiplicity = 1

Number of imaginary frequencies: 0

SCF Energy: -689.266209167 hartree

SCF Energy + ZPVE: -689.009411167 hartree

Free Energy: -689.050254 hartree

C	-2.616342785	1.195641877	4.156862042
C	-2.320888314	0.944322178	2.819185286
C	-1.827961589	1.971390426	1.999712430
C	-1.629123679	3.266616273	2.537836608
C	-1.934869391	3.489500178	3.884237253
C	-2.426696368	2.467419995	4.699480450
H	-2.997451380	0.388782293	4.776455861
H	-2.468498416	-0.045805443	2.395513241
C	-1.107822107	4.307668578	1.644145910
H	-1.785099589	4.480472151	4.302859902
H	-2.657029204	2.663153648	5.741689337
C	-0.842141094	4.002538563	0.351400448
C	-1.042913165	2.689803372	-0.225964192
H	-0.457359129	4.785016196	-0.294054899
N	-1.536289864	1.726246411	0.678694740
C	-0.881694677	5.688575820	2.188550968
H	-1.813034581	6.122276516	2.571967150
H	-0.168788591	5.675899704	3.021652119
H	-0.490093737	6.349462865	1.411678409
H	-1.696830584	0.783029480	0.354707980
C	-0.787040862	2.369908394	-1.536605894
C	-0.272020627	3.330412766	-2.515374835
C	-0.022747061	2.979620159	-3.795853381
C	-0.734214983	0.745313025	-3.388735920
C	-1.004585495	1.030475527	-2.093795338
H	-0.075013573	4.358423785	-2.236449972
H	0.358801075	3.680616911	-4.528757652
H	-0.891347222	-0.240440614	-3.811365983
H	-1.391962951	0.217178924	-1.491019481
N	-0.240898226	1.694208078	-4.251990385
H	-0.058155193	1.458813181	-5.216754969

Structure: **TS3**

Charge = 0 Multiplicity = 1

Number of imaginary frequencies: 0

SCF Energy: -839.198116000 hartree

SCF Energy + ZPVE: -838.887099000 hartree

Free Energy: -838.934380 hartree

C	1.02350600	-2.02772200	1.71121000
C	1.74833700	-3.16121200	1.01358000
C	-0.33338400	-2.52503800	2.16839300
C	1.13223200	-4.32707100	0.70943800
H	2.77434200	-2.99684700	0.70101300
C	-0.82300100	-3.73027300	1.79158500
H	-0.94399900	-1.85796000	2.77068800
H	1.68139700	-5.08320800	0.14840400
H	-1.82946400	-4.01064600	2.10227000
H	-0.37341900	-7.76117100	1.09667500
C	1.80779500	-1.59465900	2.89271000
N	2.42157900	-1.25145800	3.81397200
N	-0.15888000	-4.66939900	1.04084600
N	-0.44828000	-7.10207800	1.87176900
H	-1.36774400	-7.21654600	2.29828300
H	-0.31466400	-5.96291600	1.47395900
H	0.25630200	-7.34611600	2.56696200
C	-0.77084800	-2.69172600	-3.32230900
C	0.48685600	-2.58436200	-3.91749800
C	-1.00532500	-2.14701200	-2.06108000
C	1.51087100	-1.92230900	-3.23700500
C	1.30134200	-1.36614800	-1.97284800
C	0.02050600	-1.47883000	-1.38062500
C	0.86016100	-0.71447300	0.79757000
C	2.12978700	-0.35749800	0.07929700
C	2.35145300	-0.66869500	-1.21042000
H	-1.98319700	-2.23258500	-1.59253100
H	2.49263100	-1.84144200	-3.69591100
H	2.90394600	0.14125100	0.65885500
N	-0.21180500	-0.86601800	-0.16143700
H	-1.12093200	-1.05512700	0.24567400
H	0.59049300	0.09694000	1.48441100
C	3.65129600	-0.34338600	-1.89283900
H	4.20647200	-1.25748400	-2.13287600
H	3.48221400	0.18986200	-2.83454000
H	4.27876900	0.27823000	-1.24979100
H	0.67142500	-3.01043000	-4.89839800
H	-1.57597500	-3.20815500	-3.83758200

Structure: INT9

Charge = -1 Multiplicity = 1

Number of imaginary frequencies: 0

SCF Energy: -782.175664824 hartree

SCF Energy + ZPVE: -781.911354824 hartree

Free Energy: -781.955228 hartree

C	-5.789514822	-0.060858735	0.546789824
C	-4.446877813	0.203638616	0.803931994
C	-3.908770789	1.469756757	0.527666350
C	-4.743155405	2.483783219	-0.002486608
C	-6.087987344	2.191741831	-0.248385512
C	-6.619589760	0.928443334	0.015385419
H	-6.186748805	-1.049188334	0.760926457
H	-3.799849781	-0.566885010	1.215927239
C	-4.149244093	3.810741799	-0.241787683
H	-6.731475073	2.966448348	-0.655751012
H	-7.665056292	0.721320196	-0.188934641
C	-2.819564262	3.970979332	-0.129996546
C	-1.877976559	2.838109220	0.163962063
H	-2.374162129	4.946410113	-0.305218598
H	-1.084210628	3.187900864	0.837906532
N	-2.595407669	1.764604804	0.831556594
C	-5.053548113	4.954872300	-0.609049848
H	-5.555711025	4.763797760	-1.564509367
H	-5.835981361	5.103163503	0.143442022
H	-4.481119443	5.880501916	-0.704579055
H	-2.031972101	0.980404448	1.141215761
C	-1.141453104	2.365228459	-1.167277681
C	-0.340912027	3.490819222	-1.789918215
C	-0.748266295	4.085557948	-2.948177369
C	-2.370297958	2.542582875	-3.344002455
C	-2.088932131	1.826573972	-2.218216636
H	0.518068519	3.874692729	-1.245774942
H	-0.180853808	4.950468873	-3.298004963
H	-3.130498934	2.144485361	-4.019255381
H	-2.607651124	0.892783014	-2.018602131
C	-0.221392002	1.282258368	-0.732496746
N	0.492149042	0.436854699	-0.385254399
N	-1.782687913	3.706101200	-3.753101465

Structure: TS4

Charge = -1 Multiplicity = 1

Number of imaginary frequencies: 1

SCF Energy: -782.163198498 hartree

SCF Energy + ZPVE: -781.900079498 hartree

Free Energy: -781.943687 hartree

C	-5.831076442	-0.074705223	0.502742400
C	-4.475706458	0.187351210	0.679949856
C	-3.972652842	1.483068775	0.486056441
C	-4.853966523	2.525426051	0.111934318
C	-6.212057530	2.235205983	-0.056394348
C	-6.709597498	0.945780466	0.130972133
H	-6.201053016	-1.085000491	0.653554042
H	-3.791671994	-0.606874088	0.968607070
C	-4.292584786	3.877132925	-0.055269156
H	-6.891756696	3.033199130	-0.341548141
H	-7.765937220	0.741071698	-0.009987457
C	-2.960091880	4.045557961	-0.032308380
C	-1.979520858	2.910129881	0.117885117
H	-2.534974215	5.037418639	-0.165032026
H	-1.169922458	3.225667064	0.787654109
N	-2.642192444	1.766927632	0.723140631
C	-5.231797300	5.034737367	-0.253418793
H	-5.812300986	4.915734167	-1.175304088
H	-5.948184626	5.109627017	0.572173696
H	-4.675971841	5.972983556	-0.318534979
H	-2.043720215	0.959296002	0.862044759
C	-1.312489842	2.590535999	-1.242109956
C	-0.488189104	3.652306021	-1.801221591
C	-0.271410741	3.725599036	-3.156228309
C	-1.825426561	2.128800732	-3.597943117
C	-2.131729012	1.962000174	-2.268272924
H	0.040623967	4.324062321	-1.128926955
H	0.421743641	4.475699862	-3.537764074
H	-2.400164592	1.575764638	-4.341271285
H	-2.916570840	1.267601849	-1.980446261
C	-0.119416787	1.284269494	-0.685446641
N	0.759718706	0.521459055	-0.793269689
N	-0.877031008	2.958730097	-4.093226403

Structure: CN^-

Charge = -1 Multiplicity = 1

Number of imaginary frequencies: 0

SCF Energy: -92.928430526 hartree

SCF Energy + ZPVE: -92.923391526 hartree

Free Energy: -92.942428 hartree

C	0.274232350	2.389034793	0.040388846
N	1.386118230	2.283788047	0.401840074

Structure: **INT10**

Charge = 0 Multiplicity = 1

Number of imaginary frequencies: 0

SCF Energy: -689.278393740 hartree

SCF Energy + ZPVE: -689.020606740 hartree

Free Energy: -689.061653 hartree

C	-5.803437139	-0.032528013	0.285181869
C	-4.447507585	0.235045287	0.449059074
C	-3.972130062	1.551970149	0.370769628
C	-4.877660695	2.611321142	0.129816590
C	-6.236388432	2.315115664	-0.028033026
C	-6.706956365	1.004822543	0.041932320
H	-6.154234484	-1.058880241	0.344871929
H	-3.742770974	-0.571270717	0.637017210
C	-4.347207514	3.986587484	0.104170329
H	-6.937266924	3.125199207	-0.208151121
H	-7.763796729	0.796049727	-0.088850611
C	-3.018364289	4.177686642	0.086331030
C	-2.035083589	3.029142245	0.013778662
H	-2.603164128	5.182011990	0.062515759
H	-1.151351725	3.281607255	0.609944116
N	-2.635389603	1.839863375	0.592612981
C	-5.312060381	5.139585954	0.103223525
H	-5.933619547	5.129463325	-0.799275718
H	-5.989081975	5.090470446	0.963014824
H	-4.774081694	6.089777307	0.136354014
H	-2.023589655	1.032074194	0.634895528
C	-1.565100988	2.858184074	-1.430190132
C	-0.732206188	3.822801687	-2.005119826
C	-0.331293223	3.671180652	-3.327501257
C	-1.493810839	1.718537565	-3.543468332
C	-1.947509361	1.778823605	-2.225712271
H	-0.393592194	4.680704353	-1.430235575
H	0.320276699	4.409373820	-3.788808702
H	-1.783467816	0.884437961	-4.178322874
H	-2.581389906	0.986364712	-1.840719845
N	-0.701074695	2.639614606	-4.099334095

Structure: TS5

Charge = -1 Multiplicity = 1

Number of imaginary frequencies: 1

SCF Energy: -782.168126497 hartree

SCF Energy + ZPVE: -781.910934497 hartree

Free Energy: -781.954818 hartree

C	-6.056279974	0.235406910	1.228739461
C	-4.875421107	0.344057701	0.488901682
C	-4.467983252	1.578052496	-0.028077532
C	-5.255777748	2.732180987	0.212240273
C	-6.433504338	2.596432372	0.950204392
C	-6.843950720	1.358316703	1.460917293
H	-6.351862066	-0.733929630	1.620207264
H	-4.260773571	-0.533682088	0.303159496
C	-4.787374935	4.025788375	-0.320306969
H	-7.042657895	3.476091016	1.137860003
H	-7.763346854	1.282100285	2.032843318
C	-3.570220201	4.083772776	-0.909422053
C	-2.682522507	2.943367853	-1.043399710
H	-3.214447641	5.044491673	-1.273884068
H	-1.816732527	2.992746107	0.178769359
N	-3.326606753	1.659501423	-0.825865502
C	-5.662555257	5.237486247	-0.167730175
H	-6.640632570	5.090913782	-0.642863473
H	-5.854828160	5.467386238	0.887971421
H	-5.189555937	6.111381269	-0.623407955
H	-2.676912521	0.900491292	-0.640247456
C	-1.541886929	2.954178288	-1.903828056
C	-0.841901593	4.151545300	-2.233070815
C	0.339705231	4.094728348	-2.944435383
C	0.283853485	1.826895174	-3.057970649
C	-0.908571814	1.761442341	-2.348709148
H	-1.216681301	5.122540096	-1.925793814
H	0.856066457	5.020614805	-3.191538916
H	0.745949568	0.901911612	-3.399958562
H	-1.350763364	0.785490675	-2.179213745
N	0.929755616	2.958099525	-3.372853153
C	-1.158521141	2.813163570	1.285718859
N	-0.619424191	2.768222269	2.314904803

Structure: HCN

Charge = 0 Multiplicity = 1

Number of imaginary frequencies: 0

SCF Energy: -93.391984157 hartree

SCF Energy + ZPVE: -93.378253157 hartree

Free Energy: -93.391906 hartree

H	-1.051789369	3.872500390	0.628196794
C	-0.068751982	4.383364948	0.883918367
N	0.941382351	4.907887662	1.146375840

Structure: INT11

Charge = -1 Multiplicity = 1

Number of imaginary frequencies: 0

SCF Energy: -688.772093742 hartree

SCF Energy + ZPVE: -688.529452742 hartree

Free Energy: -688.570183 hartree

C	-6.058890797	0.233758464	1.225184058
C	-4.899175167	0.340110108	0.446368655
C	-4.506781596	1.573060118	-0.085270196
C	-5.278600222	2.735900402	0.190453362
C	-6.428575855	2.600803822	0.972081867
C	-6.830671271	1.358283896	1.488400653
H	-6.346725429	-0.736495793	1.620446542
H	-4.295654520	-0.539935030	0.236486974
C	-4.808217513	4.021994213	-0.338064387
H	-7.024421007	3.483057737	1.188484460
H	-7.731398562	1.284781254	2.089987605
C	-3.609645180	4.064002600	-0.988814998
C	-2.802500932	2.920659709	-1.262207435
H	-3.246032693	5.030089952	-1.330126976
N	-3.399230216	1.661277223	-0.912964055
C	-5.624223260	5.256752967	-0.085060660
H	-6.637077868	5.170077948	-0.500852422
H	-5.744041060	5.454870650	0.989043678
H	-5.147941059	6.131131348	-0.537282314
H	-2.774866819	0.867578517	-0.851731205
C	-1.577567539	2.943322213	-1.918206194
C	-0.892774774	4.153980569	-2.322906745
C	0.321378850	4.099940899	-2.960593556
C	0.374648250	1.829367058	-2.917346516
C	-0.843287630	1.747195553	-2.274023544
H	-1.320528053	5.130425340	-2.118436942
H	0.804341658	5.035042165	-3.243906122
H	0.892482551	0.902836488	-3.167891167
H	-1.231013124	0.756282157	-2.059956669
N	1.005299836	2.966899453	-3.280831751

Structure: INT12

Charge = 0 Multiplicity = 2

Number of imaginary frequencies: 0

SCF Energy: -688.672674813 hartree

SCF Energy + ZPVE: -688.427444813 hartree

Free Energy: -688.468281 hartree

C	-6.048762514	0.233447467	1.199230319
C	-4.848990443	0.352816348	0.508137768
C	-4.448503203	1.604302134	0.018881503
C	-5.252420173	2.751571225	0.225572384
C	-6.460856734	2.596810271	0.925975619
C	-6.859634099	1.354400802	1.408927716
H	-6.353759245	-0.738305411	1.575411779
H	-4.212736489	-0.511673282	0.338255126
C	-4.785630444	4.025458121	-0.294158546
H	-7.090424347	3.465370996	1.092353427
H	-7.796508246	1.256947603	1.947993532
C	-3.587825309	4.067586723	-0.964496319
C	-2.785296933	2.923674443	-1.178547629
H	-3.252610630	5.016423453	-1.368909650
N	-3.260359021	1.728392368	-0.670942996
C	-5.618265937	5.257117239	-0.099946975
H	-6.608433014	5.143441545	-0.557436495
H	-5.779836313	5.463295391	0.964908648
H	-5.130588317	6.125808616	-0.547734109
H	-2.683383893	0.897862263	-0.728965363
C	-1.545185607	2.931433298	-1.910659970
C	-0.888824650	4.136564457	-2.265353584
C	0.304106512	4.092742531	-2.963759280
C	0.304144943	1.817009087	-3.017746297
C	-0.892839491	1.742437695	-2.320101094
H	-1.288386157	5.104157117	-1.984356864
H	0.802830594	5.023037331	-3.226158915
H	0.793556248	0.897712674	-3.332267062
H	-1.307421485	0.757115761	-2.133875440
N	0.921153397	2.960093734	-3.349767235

Structure: **TS6**

Charge = 0 Multiplicity = 2

Number of imaginary frequencies: 1

SCF Energy: -745.203464040 hartree

SCF Energy + ZPVE: -744.925073040 hartree

Free Energy: -744.969045 hartree

C	-6.09073800	0.32635800	1.23634100
C	-4.87063800	0.44837800	0.58637700
C	-4.44473400	1.69675000	0.07564900

C	-5.30146200	2.82593600	0.21660800
C	-6.53445700	2.67061900	0.87358300
C	-6.93028600	1.43871800	1.38749900
H	-6.40003900	-0.64290500	1.61746500
H	-4.23352100	-0.41947600	0.43741600
C	-4.84721500	4.08493500	-0.34290900
H	-7.18721100	3.53159000	0.98438800
H	-7.88426000	1.34030900	1.89594700
C	-3.65672800	4.09337300	-1.02109700
C	-2.84841000	2.93099300	-1.14896300
H	-3.34232600	5.00908900	-1.51352100
N	-3.20696300	1.78362800	-0.50389100
C	-5.68626500	5.32070600	-0.19911400
H	-6.70007300	5.16617500	-0.58697900
H	-5.78877600	5.60933000	0.85434200
H	-5.23662500	6.15670600	-0.74003600
H	-2.27019300	0.98905300	0.04464800
C	-1.59441600	2.94806600	-1.85419800
C	-0.91887200	4.14069600	-2.22886100
C	0.26800000	4.07027400	-2.93441300
C	0.22454400	1.79184100	-2.98050900
C	-0.96156300	1.74420800	-2.26857500
H	-1.29425000	5.11648300	-1.93994800
H	0.78399600	4.99052300	-3.20135100
H	0.69023800	0.86325300	-3.30562600
H	-1.42669900	0.78237800	-2.07778500
N	0.86482500	2.92482500	-3.32411100
N	-1.42658700	0.28155800	0.61611800
H	-1.09640000	-0.49709500	0.04525300
H	-1.84198700	-0.11378000	1.46005200
H	-0.61297000	0.83261800	0.89212100

Structure: INT13

Charge = -1 Multiplicity = 2

Number of imaginary frequencies: 0

SCF Energy: -688.187140108 hartree

SCF Energy + ZPVE: -687.955661108 hartree

Free Energy: -687.996217 hartree

C	-6.077426551	0.219825968	1.092071711
C	-4.891116874	0.344997905	0.390741484
C	-4.431165250	1.611937989	-0.070393005
C	-5.243742915	2.758082434	0.217340749
C	-6.444280247	2.599799202	0.932133213

C	-6.867500176	1.348634626	1.371383725
H	-6.399578776	-0.761773650	1.430255360
H	-4.278040922	-0.526293266	0.174268744
C	-4.767733439	4.040873071	-0.257762561
H	-7.052534993	3.474934960	1.145230657
H	-7.797280182 1.246309746 1.922357561		
C	-3.584424105	4.072381009	-0.939945698
C	-2.820670344	2.885400813	-1.190799158
H	-3.221136958	5.030613361	-1.300155916
N	-3.260979794	1.670983468	-0.749924292
C	-5.566065133	5.286301010	0.002353782
H	-6.569167460	5.216487474	-0.435560786
H	-5.699846335	5.458142501	1.077272038
H	-5.067038634	6.160094007	-0.424101293
C	-1.576224625	2.932568075	-1.909177278
C	-0.989287907	4.126068735	-2.425689383
C	0.210953245	4.076252049	-3.106861667
C	0.373606558	1.817711264	-2.858619898
C	-0.818966525	1.749621543	-2.164046589
H	-1.463010403 5.093603829	-2.298490237	
H	0.640167208	4.999496678	-3.492716106
H	0.935142734	0.902658320	-3.042423610
H	-1.179600359 0.790044185	-1.812260644	
N	0.922171160	2.950803694	-3.345769902

Structure: 3ea

Charge = 0 Multiplicity = 1

Number of imaginary frequencies: 0

SCF Energy: -688.096726629 hartree

SCF Energy + ZPVE: -687.862336629 hartree

Free Energy: -687.902386 hartree

C	-5.937501629	0.258169665	1.255488939
C	-4.758184084	0.391535780	0.564016616
C	-4.380548826	1.649940453	0.022519137
C	-5.234185195	2.772892338	0.206440184
C	-6.446832643	2.604274135	0.926045128
C	-6.790452906	1.375072605	1.438181929
H	-6.221700398	-0.706150827	1.665621480
H	-4.090345171	-0.451511714	0.412389090
C	-4.827080773	4.023906740	-0.353818887
H	-7.105123248	3.455437411	1.069500488
H	-7.719936994	1.255983157	1.986355287
C	-3.632673098	4.062634017	-1.031307071

C	-2.842843632	2.887021808	-1.162152806
H	-3.302436002	4.990869865	-1.485827159
N	-3.202023224	1.724297222	-0.658823363
C	-5.684104106	5.247691454	-0.211365998
H	-6.669817707	5.087613348	-0.660595029
H	-5.842357284	5.491692274	0.844287448
H	-5.214687477	6.104139612	-0.699003124
C	-1.551366127	2.923207275	-1.906342525
C	-0.814708547	4.100913938	-2.060632138
C	0.387731863	4.058122626	-2.762343589
C	0.177436600	1.820403325	-3.161812974
C	-1.030044845	1.756791430	-2.474811773
H	-1.144877243	5.041148590	-1.632380180
H	0.975811443	4.964277796	-2.884175020
H	0.593279153	0.924019271	-3.615036782
H	-1.562310212	0.816115426	-2.388237918
N	0.887104312	2.946051979	-3.311468391

Structure: **TSS1**

Charge = 0 Multiplicity = 1

Number of imaginary frequencies: 1

SCF Energy: -782.523330951 hartree

SCF Energy + ZPVE: -782.255123951 hartree

Free Energy: -782.298793 hartree

C	0.642197037	-4.323148920	-0.796574728
C	1.872638361	-4.851899841	-0.087641583
C	0.462252041	-5.015345171	-2.134528778
C	2.760396964	-5.650981011	-0.703662342
H	2.040204096	-4.546939836	0.939839683
C	1.417107741	-5.804891282	-2.656006615
H	-0.451521681	-4.829604726	-2.686159363
H	3.656944314	-6.000095946	-0.203676866
H	1.302002234	-6.270098102	-3.628637826
N	2.591976482	-6.084364179	-1.997886187
C	-1.831084777	0.896018109	-2.845366088
C	-0.678636302	1.467219025	-3.402332829
C	-1.771143558	-0.323086330	-2.185858932
C	0.528225519	0.784646499	-3.298876775
C	0.613899916	-0.445959092	-2.631481767
C	-0.549319954	-1.015962052	-2.045252778
C	0.717656467	-2.783827252	-1.066122535
C	1.895983796	-2.361305019	-1.853737726
C	1.852380104	-1.231942100	-2.587538903

H	-2.664982053	-0.766146500	-1.754950983
H	1.422109137	1.210205844	-3.746390772
H	2.786008331	-2.982506802	-1.814909952
N	-0.559114050	-2.222112174	-1.374608060
H	0.176967989	-2.061333912	-0.107496216
H	1.029864478	-2.405893646	0.201398771
C	3.042934246	-0.784030778	-3.383237834
H	2.787458978	-0.679985645	-4.442831764
H	3.390477837	0.195085887	-3.035770479
H	3.863863723	-1.497221543	-3.285648734
H	-0.727422035	2.422360711	-3.914923031
H	-2.784210008 1.411818050	-2.926212318	
C	-0.548629588	-4.580189317	0.053743762
N	-1.446016719	-4.836056899	0.737541156
H	3.244573666	-6.745494151	-2.394490637

Structure: INTS1

Charge = 0 Multiplicity = 1

Number of imaginary frequencies: 0

SCF Energy: -781.487296587 hartree

SCF Energy + ZPVE: -781.232288587 hartree

Free Energy: -781.276421 hartree

C	0.449063655	-3.967582148	-0.026086753
C	1.616627326	-3.990048756	0.951953350
C	0.419543668	-5.263892535	-0.825067340
C	2.501558668	-4.999729172	0.997692455
H	1.732175855	-3.138749065	1.613751040
C	1.360290467	-6.214203092	-0.695814918
H	-0.388921215	-5.395962530	-1.535667722
H	3.340322419	-4.989576374	1.685058763
H	1.336192784	-7.121753870	-1.288769861
C	-0.814531630	-3.865578554	0.751020711
N	-1.775870640	-3.864684199	1.395165562
N	2.413868499	-6.103875419	0.181934069
C	-1.268977947	1.296216941	-2.559619314
C	-0.180920386	1.468345484	-3.448602236
C	-1.324979031	0.196175007	-1.736603152
C	0.832136002	0.538033000	-3.497290073
C	0.801505808	-0.607127531	-2.659211557
C	-0.293747676	-0.776857031	-1.769934746
C	0.550085489	-2.752044438	-0.961493746
C	1.686002749	-2.671754905	-1.811417773
C	1.827957194	-1.607733161	-2.666121162

H	-2.150636074	0.044332087	-1.047388093
H	1.663376711	0.676695397	-4.181677273
H	2.435312308	-3.458092092	-1.776182135
N	-0.400977159 -1.854268423 -0.931242806		
C	3.013513629	-1.488491558	-3.578269333
H	2.697770276	-1.458859644	-4.626311972
H	3.567546799	-0.565379178	-3.378288698
H	3.688455072	-2.335539484	-3.442240767
H	-0.148182964	2.340410931	-4.094432423
H	-2.061314216	2.038053115	-2.530414483
H	3.084419450	-6.853517371	0.267867745

Structure: **TSS2**

Charge = 0 Multiplicity = 1

Number of imaginary frequencies: 1

SCF Energy: -689.138649852 hartree

SCF Energy + ZPVE: -688.891891852 hartree

Free Energy: -688.920135 hartree

C	1.136294824	-3.998550434	-0.220285171
C	2.062819601	-4.270264761	0.785535903
C	0.437693612	-5.056525666	-0.790292583
C	2.248254140	-5.591687600	1.177336346
H	2.625428418	-3.471625987	1.261981607
C	0.701726737	-6.346634168	-0.329207687
H	-0.293381162	-4.880187088	-1.570803988
H	2.959871918	-5.833485523	1.962265690
H	0.172354004	-7.194636808	-0.756120799
N	1.585500718	-6.621298193	0.634231792
C	-1.915654271	0.302358822	-3.305125498
C	-0.820109886	1.085042726	-3.698796440
C	-1.733773896	-0.836825243	-2.536359029
C	0.457855539	0.691769320	-3.322127508
C	0.666015451	-0.453404818	-2.537246682
C	-0.445233965	-1.234585637	-2.115272784
C	0.939881833	-2.589593598	-0.735879210
C	2.139741580	-1.992054773	-1.369936034
C	2.006543507	-0.953977113	-2.220333633
H	-2.582455195	-1.443898794	-2.232922094
H	1.313875630	1.278673781	-3.643334113
H	3.110288166	-2.411471794	-1.124037902
N	-0.336206502	-2.377728316	-1.350734766
H	0.055740913	-1.922674721	-0.013805220
H	0.892352456	-1.955052348	0.475622920

C	3.206259985	-0.328233533	-2.868135913
H	3.116079145	-0.348164871	-3.959000681
H	3.297979205	0.721649437	-2.568962641
H	4.119827208	-0.850926598	-2.578160383
H	-0.966365686	1.978281882	-4.297238484
H	-2.920713266	0.590252477	-3.601753304

Structure: **INTS2**

Charge = 0 Multiplicity = 1

Number of imaginary frequencies: 0

SCF Energy: -688.096773033 hartree

SCF Energy + ZPVE: -687.862201033 hartree

Free Energy: -687.902002 hartree

C	1.040633970	-4.151070142	-0.519455025
C	2.082346848	-4.452284713	0.362055539
C	0.008662157	-5.085729912	-0.645803043
C	2.044988092	-5.654798712	1.063993279
H	2.904988514	-3.764510528	0.527718261
C	0.068073025	-6.261205192	0.095208959
H	-0.822245877	-4.902917241	-1.318255046
H	2.843337285	-5.901024019	1.759499628
H	-0.721451722 -7.002858906	0.002920137	
N	1.064011602	-6.554995118	0.940772375
C	-1.648045073	0.399002827	-3.419067699
C	-0.495438338	1.128860914	-3.802599563
C	-1.524522250	-0.769194495	-2.707127311
C	0.758871526	0.675292659	-3.467442730
C	0.918203163	-0.529002072	-2.731864251
C	-0.240320736	-1.259956884	-2.347849031
C	1.010258233	-2.880387450	-1.296960829
C	2.223152278	-2.223980519	-1.644100708
C	2.196161565	-1.051736125	-2.359637426
H	-2.395030901	-1.343198921	-2.402965911
H	1.637764882	1.239292604	-3.764102628
H	3.174972439	-2.662348641	-1.361641566
N	-0.176218268	-2.423729426	-1.639882789
C	3.461672614	-0.343872399	-2.746284392
H	3.539288698	-0.248662187	-3.834319126
H	3.485094961	0.667853559	-2.328063054
H	4.333440806	-0.890447569	-2.381676189
H	-0.607029157	2.051319567	-4.364054383
H	-2.631980046	0.768810171	-3.691117698

Characterization data of products

2-(Pyridin-4-yl)quinoline (3aa)

(Hey and Williams, 1950, Nunn and Schofield, 1952; Kouznetsov et al., 2012, 2017; Yamaguchi et al., 2016; Pang et al., 2017; Zhang et al., 2017a, 2017b; Roder et al., 2019) yellow oil was obtained by column chromatography (eluent: EtOAc/petroleum ether = 1/4) with 21% isolated yield (10.8 mg). ^{1}H NMR (500 MHz, $CDCl_3$) δ 8.79 (d, J = 5.1 Hz, 2H), 8.30 (d, J = 8.6 Hz, 1H), 8.20 (d, J = 8.5 Hz, 1H), 8.08 (d, J = 5.9 Hz, 2H), 7.92 (d, J = 8.5 Hz, 1H), 7.87 (d, J = 8.1 Hz, 1H), 7.78 (t, J = 7.7 Hz, 1H), 7.60 (t, J = 7.5 Hz, 1H). ^{13}C NMR (126 MHz, $CDCl_3$) δ 154.4, 150.4, 148.3, 146.7, 137.3, 130.1, 130.0, 127.8, 127.5, 127.2, 121.6, 118.4.

4-(Pyridin-4-yl)quinoline (3aa′)

(Hey and Williams, 1950, Nunn and Schofield, 1952; Kouznetsov et al., 2012, 2017; Yamaguchi et al., 2016; Pang et al., 2017; Zhang et al., 2017a, 2017b; Roder et al., 2019) yellow oil was obtained by column chromatography (eluent: EtOAc/petroleum ether = 1/4) with 51% isolated yield (26.4 mg). ^{1}H NMR (500 MHz, $CDCl_3$) δ 8.99 (d, J = 4.3 Hz, 1H), 8.80 (d, J = 4.4 Hz, 2H), 8.22 (d, J = 8.5 Hz, 1H), 7.83 (d, J = 8.5 Hz, 1H), 7.78 (t, J = 7.6 Hz, 1H), 7.56 (t, J = 7.6 Hz, 1H), 7.45 (d, J = 4.8 Hz, 2H), 7.34 (d, J = 4.3 Hz, 1H). ^{13}C NMR (126 MHz, $CDCl_3$) δ 150.1, 149.9, 148.6, 145.9, 145.5, 130.1, 129.7, 127.3, 125.7, 125.0, 124.2, 120.9.

2-Methyl-4-(pyridin-4-yl)quinoline (3ba)

(Hey and Williams, 1950, Nunn and Schofield, 1952; Kouznetsov et al., 2012, 2017; Yamaguchi et al., 2016; Pang et al., 2017; Zhang et al., 2017a, 2017b; Roder et al., 2019) yellow oil was obtained by column chromatography (eluent: EtOAc/petroleum ether = 1/4) with 67% isolated yield (36.9 mg). ^{1}H NMR (500 MHz, $CDCl_3$) δ 8.78 (d, J = 5.6 Hz, 2H), 8.12 (d, J = 8.4 Hz, 1H), 7.74 (m, 2H), 7.48 (t, J = 7.6 Hz, 1H), 7.44 (d, J = 5.9 Hz, 2H), 7.23 (s, 1H), 2.80 (s, 3H).^{13}C NMR (126 MHz, $CDCl_3$) δ 158.5, 149.9, 148.2, 146.1, 145.6, 129.7, 129.2, 126.3, 124.7, 124.3, 122.6, 121.8, 25.3.

2-Phenyl-4-(pyridin-4-yl)quinoline (3ca)

yellow solid was obtained by column chromatography (eluent: EtOAc/petroleum ether = 1/4) with 51% isolated yield (36.0 mg). m. p. = 112-114°C. ^{1}H NMR (500 MHz, $CDCl_3$) δ 8.81 (d, J = 5.1 Hz, 2H), 8.27 (d, J = 8.4 Hz, 1H), 8.19 (d, J = 7.2 Hz, 2H), 7. 78 (m, 3H), 7.52 (m, 6H). ^{13}C NMR (126 MHz, $CDCl_3$) δ 156.9, 150.1, 148.7, 146.3, 146.2, 139.2, 130.4, 129.9, 129.6, 128.9, 127.5, 126.9, 124.8, 124.7, 124.3, 118.9. HRMS (ESI) *m/z:* $[M + H]^+$ calcd for $C_{20}H_{14}N_2$: 283.1230, found:283.1229.

3-Chloro-2-(pyridin-4-yl)quinolone and 3-chloro-4-(pyridin-4-yl)quinolone (3da)

(Hey and Williams, 1950, Nunn and Schofield, 1952; Kouznetsov et al., 2012, 2017; Yamaguchi et al., 2016; Pang et al., 2017; Zhang et al., 2017a, 2017b; Roder et al., 2019) yellow oil was obtained by column chromatography (eluent: EtOAc/petroleum ether = 1/4) with 52% isolated yield (31.3 mg). ^{1}H NMR (500 MHz, Chloroform-*d*) δ 9.07 (s, 1H), 8.82 (d, J = 26.3 Hz, 4H), 8.23 (s, 1H), 8.17 (d, J = 8.6 Hz, 1H), 8.00 (m, 2H), 7.83 (dd, J = 9.0, 2.2 Hz, 1H), 7.75 (m, 3H), 7.51 (m, 1H), 7.40 (d, J = 8.2 Hz, 1H), 7.30 (d, J = 5.5 Hz, 2H). ^{13}C NMR (126 MHz, Chloroform-*d*) δ 151.9, 150.2, 149.7, 149.7, 146.7, 145.6, 144.9, 135.6, 133.9, 131.3, 129.9, 129.8, 129.1, 128.6, 128.1, 127.9, 125.4, 124.2, 124.0, 122.4.

4-Methyl-2-(pyridin-4-yl)quinoline (3ea)

(Hey and Williams, 1950, Nunn and Schofield, 1952; Kouznetsov et al., 2012, 2017; Yamaguchi et al., 2016; Pang et al., 2017; Zhang et al., 2017a, 2017b; Roder et al., 2019) yellow oil was obtained by column chromatography (eluent: EtOAc/petroleum ether = 1/4) with 93% isolated yield (51.2 mg). ^{1}H NMR (500 MHz, $CDCl_3$) δ 8.77 (d, J = 6.0 Hz, 2H), 8.18 (d, J = 8.4 Hz, 1H), 8.04 (d, J = 4.6 Hz, 2H), 8.01 (d, J = 8.3 Hz, 1H), 7.75 (t, J = 7.6 Hz, 1H), 7.72 (s, 1H), 7.59 (t, J = 7.6 Hz, 1H), 2.78 (s, 3H). ^{13}C NMR (126 MHz, $CDCl_3$) δ 154.1, 150.4, 148.0, 146.8, 145.5, 130.5, 129.7, 127.8, 126.9, 123.7, 121.6, 119.2, 19.0.

5-Chloro-2-(pyridin-4-yl)quinoline (3fa)

yellow solid was obtained by column chromatography (eluent: EtOAc/petroleum ether = 1/4) with 76% isolated yield (45.7 mg). m. p. = 123-125°C. ^{1}H NMR (500 MHz, $CDCl_3$) δ 8.80 (d, J = 5.1 Hz, 2H), 8.69 (d, J = 8.8 Hz, 1H), 8.12 (d, J = 7.9 Hz, 1H), 8.08 (d, J = 5.8 Hz, 2H), 8.00 (d, J = 8.8 Hz, 1H), 7.71 (m, 2H). ^{13}C NMR (126 MHz, $CDCl_3$) δ 155.1, 150.5, 148.9, 146.0, 134.3, 131.3, 129.8, 129.1, 127.1, 126.0, 121.6, 119.2. HRMS (ESI) *m/z:* $[M + H]^+$ calcd for $C_{14}H_9ClN_2$: 241.0527, found: 241.0521

5-Bromo-2-(pyridin-4-yl)quinoline (3ga)

yellow solid was obtained by column chromatography (eluent: EtOAc/petroleum ether = 1/4) with 84% isolated yield (59.9 mg). m. p. = 142-144°C. ^{1}H NMR (500 MHz, $CDCl_3$) δ 8.80 (d, *J* = 5.0 Hz, 2H), 8.65 (d, *J* = 8.8 Hz, 1H), 8.15 (d, *J* = 8.5 Hz, 1H), 8.07 (d, *J* = 4.7 Hz, 2H), 7.98 (d, *J* = 8.8 Hz, 1H), 7.85 (d, *J* = 7.5 Hz, 1H), 7.61 (t, 1H). ^{13}C NMR (126 MHz, $CDCl_3$) δ 155.1, 150.5, 148.9, 145.9, 136.9, 130.8, 130.3, 129.9, 127.3, 121.8, 121.7, 119.5. HRMS (ESI) *m/z:* [M + H] $^+$ calcd for $C_{14}H_9BrN_2$: 285.0022, found: 285.0020.

6-Fluoro-2-(pyridin-4-yl)quinoline (3ha)

yellow oil was obtained by column chromatography (eluent: EtOAc/petroleum ether = 1/4) with 23% isolated yield (13.0 mg). ^{1}H NMR (500 MHz, $CDCl_3$) δ 8.80 (s, 2H), 8.26 (d, *J* = 8.6 Hz, 1H), 8.20 (dd, *J* = 9.2, 5.3 Hz, 1H), 8.08 (d, *J* = 5.6 Hz, 2H), 7.94 (d, *J* = 8.6 Hz, 1H), 7.57 (m, 1H), 7.49 (d, *J* = 8.7 Hz, 1H). ^{13}C NMR (126 MHz, $CDCl_3$) δ 160.9 (d, *J* = 249.6 Hz), 153.7 (d, *J* = 3.0 Hz), 150.2, 146.7, 145.4, 136.7, 132.5 (d, *J* = 9.2 Hz), 128.5 (d, *J* = 10.2 Hz), 121.4, 120.5 (d, *J* = 21.3 Hz), 119.1, 110.6 (d, *J* = 21.8 Hz). ^{19}F NMR (471 MHz, $CDCl_3$) δ -111.9. HRMS (ESI) *m/z:* [M + H] $^+$ calcd for $C_{14}H_9FN_2$: 225.0823, found: 225.0822.

6-Fluoro-4-(pyridin-4-yl)quinoline (3ha′)

white solid was obtained by column chromatography (eluent: EtOAc/petroleum ether = 1/4) with 57% isolated yield (31.8 mg). m. p. = 137-139°C. ^{1}H NMR (500 MHz, $CDCl_3$) δ 8.96 (d, *J* = 4.3 Hz, 1H), 8.82 (d, *J* = 5.7 Hz, 2H), 8.24 (m, 1H), 7.57 (m, 1H), 7.46 (m, 3H), 7.37 (d, *J* = 4.3 Hz, 1H). ^{13}C NMR (126 MHz, $CDCl_3$) δ 160.9 (d, *J* = 249.1 Hz), 150.3, 149.2 (d, *J* = 2.7 Hz), 145.7, 145.3, 144.9, 132.7 (d, *J* = 9.3 Hz), 126.5 (d, *J* = 9.6 Hz), 124.0, 121.5, 120.0 (d, *J* = 25.7 Hz), 108.4 (d, *J* = 23.3 Hz). ^{19}F NMR (471 MHz, $CDCl_3$) δ -111.1 (s).HRMS (ESI) *m/z:* [M + H] $^+$ calcd for $C_{14}H_9FN_2$: 225.0823, found: 225.0823.

7-Chloro-2-(pyridin-4-yl)quinoline (3ia)

yellow solid was obtained by column chromatography (eluent: EtOAc/petroleum ether = 1/4) with 29% isolated yield (17.5 mg). m. p. = 152-154°C. ^{1}H NMR (500 MHz, $CDCl_3$) δ 8.80 (d, *J* = 4.2 Hz, 2H), 8.28 (d, *J* = 8.5 Hz, 1H), 8.20 (s, 1H), 8.07 (d, *J* = 4.8 Hz, 2H), 7.92 (d, *J* = 8.4 Hz, 1H), 7.81 (d, *J* = 8.6 Hz, 1H), 7.55 (d, *J* = 8.7 Hz, 1H). ^{13}C NMR (126 MHz, $CDCl_3$) δ 155.3, 150.4, 148.6, 146.3, 137.1, 136.0, 128.9, 128.7, 128.3, 126.2, 121.6, 118.6. HRMS (ESI) *m/z:* [M + H] $^+$ calcd for $C_{14}H_9ClN_2$: 241.0527, found: 241.0525.

7-Chloro-4-(pyridin-4-yl)quinoline (3ia′)

yellow solid was obtained by column chromatography (eluent: EtOAc/petroleum ether = 1/4) with 55% isolated yield (33.1 mg). m. p. = 153-155°C. ^{1}H NMR (500 MHz, $CDCl_3$) δ 8.99 (d, *J* = 4.2 Hz, 1H), 8.81 (d, *J* = 4.1 Hz, 2H), 8.20 (s, 1H), 7.76 (d, *J* = 9.0 Hz, 1H), 7.50 (d, *J* = 9.0 Hz, 1H), 7.43 (d, *J* = 4.3 Hz, 2H), 7.34 (d, *J* = 4.3 Hz, 1H). ^{13}C NMR (126 MHz, $CDCl_3$) δ 150.9, 150.4, 150.2, 149.0, 145.6, 145.3, 135.8, 129.0, 128.3, 126.4, 124.1, 121.0. HRMS (ESI) *m/z:* [M + H] $^+$ calcd for $C_{14}H_9ClN_2$: 241.0527, found: 241.0515.

2,6-Dimethyl-4-(pyridin-4-yl)quinoline (3ja)

yellow oil was obtained by column chromatography (eluent: EtOAc/petroleum ether = 1/4) with 71% isolated yield (41.6 mg). ^{1}H NMR (500 MHz, $CDCl_3$) δ 8.78 (d, *J* = 4.8 Hz, 2H), 8.00 (d, *J* = 8.6 Hz, 1H), 7.55 (d, *J* = 8.6 Hz, 1H), 7.49 (s, 1H), 7.42 (d, *J* = 4.8 Hz, 2H), 7.17 (s, 1H), 2.77 (s, 3H), 2.46 (s, 3H). ^{13}C NMR (126 MHz, $CDCl_3$) δ 157.4, 150.0, 146.8, 146.3, 144.9, 136.2, 131.9, 128.9, 124.2, 124.0, 123.5, 121.8, 25.1, 21.7. HRMS (ESI) *m/z:* [M + H] $^+$ calcd for $C_{16}H_{14}N_2$: 235.1230, found: 235.1224.

6-Bromo-2-methyl-4-(pyridin-4-yl)quinoline (3ka)

yellow solid was obtained by column chromatography (eluent: EtOAc/petroleum ether = 1/4) with 56% isolated yield (41.9 mg). m. p. = 163-165°C. ^{1}H NMR (500 MHz, $CDCl_3$) δ 8.81 (d, *J* = 4.9 Hz, 2H), 7.97 (d, *J* = 9.0 Hz, 1H), 7.87 (s, 1H), 7.79 (d, *J* = 9.0 Hz, 1H), 7.41 (d, *J* = 5.5 Hz, 2H), 7.24 (s, 1H), 2.78 (s, 3H). ^{13}C NMR (126 MHz, $CDCl_3$) δ 159.0, 150.2, 146.9, 145.3, 144.7, 133.2, 131.0, 126.9, 125.3, 124.1, 122.6, 120.4, 25.3. HRMS (ESI) *m/z:* [M + H] $^+$ calcd for $C_{15}H_{11}BrN_2$: 299.0178, found: 299.0172.

8-Methyl-2-(pyridin-4-yl)quinoline (3la)

yellow oil was obtained by column chromatography (eluent: EtOAc/petroleum ether = 1/4) with 27% isolated yield (14.9 mg). ^{1}H NMR (500 MHz, $CDCl_3$) δ 8.78 (d, *J* = 4.6 Hz, 2H), 8.26 (d, *J* = 8.5 Hz, 1H), 8.15 (d, *J* = 5.9 Hz, 2H), 7.93 (d, *J* = 8.5 Hz, 1H), 7.70 (d, *J* = 7.8 Hz, 1H), 7.61 (d, *J* = 6.9 Hz, 1H), 7.50–7.45 (m, 1H), 2.91 (s, 3H). ^{13}C NMR (126 MHz, $CDCl_3$) δ 152.6, 150.4, 147.2, 146.8, 138.0, 137.4, 130.1, 127.8, 127.0, 125.4, 121.5, 117.7, 17.8. HRMS (ESI) *m/z:* [M + H] $^+$ calcd for $C_{15}H_{12}N_2$: 221.1073, found: 221.1044.

8-Methyl-4-(pyridin-4-yl)quinolone/8-methyl-6-(pyridin-4-yl)quinoline (3la′, C4: C6 = 1/1)

yellow oil was obtained by column chromatography (eluent: EtOAc/petroleum ether = 1/4) with 40% isolated yield (22.0 mg). ^{1}H NMR (500 MHz, Chloroform-*d*) δ 8.99 (dd, *J* = 7.6, 4.3 Hz, 2H), 8.78 (dd, *J* = 11.7, 5.1 Hz, 4H), 7.75 (s, 1H), 7.70 (s, 1H), 7.62 (dd, *J* = 11.8, 7.7 Hz, 2H), 7.41 (dd, *J* = 13.3, 5.5 Hz, 6H), 7.31 (t, *J* = 4.3 Hz, 2H), 2.86 (s, 3H), 2.83 (s, 3H). ^{13}C NMR (126 MHz, Chloroform-*d*) δ 150.2, 149.9, 148.8, 148.6, 147.6, 146.4, 145.6, 144.8, 140.2, 137.8, 133.2, 129.9, 126.9, 125.7, 125.1, 123.0, 121.5, 121.2, 120.7, 18.5, 18.2. HRMS (ESI) *m/z:* [M + H] $^+$ calcd for $C_{15}H_{12}N_2$: 221.1073, found: 221.1069.

8-Fluoro-2-(pyridin-4-yl)quinoline (3ma)

yellow oil was obtained by column chromatography (eluent: EtOAc/petroleum ether = 1/4) with 23% isolated yield (12.9 mg). ^{1}H NMR (500 MHz, $CDCl_3$) δ 8.79 (d, *J* = 5.3 Hz, 2H), 8.32 (d, *J* = 8.6 Hz, 1H), 8.10 (d, *J* = 5.8 Hz, 2H), 7.98 (d, *J* = 8.6 Hz, 1H), 7.66 (d, *J* = 8.1 Hz, 1H), 7.55 (m, 1H), 7.49 (m, 1H). ^{13}C NMR (126 MHz, $CDCl_3$) δ 158.33 (d, *J* = 258.1 Hz), 154.5, 150.5, 146.1, 138.5 (d, *J* = 11.6 Hz), 137.1, 129.3 (d, *J* = 1.8 Hz), 127.0 (d, *J* = 8.0 Hz), 123.2 (d, *J* = 4.8 Hz), 121.6, 119.3, 114.2 (d, *J* = 19.0 Hz). ^{19}F NMR (471 MHz, $CDCl_3$) δ -124.6. HRMS (ESI) *m/z:* [M + H] $^+$ calcd for $C_{14}H_9FN_2$: 225.0823, found: 225.0826.

8-Fluoro-4-(pyridin-4-yl)quinoline (3ma′)

yellow solid was obtained by column chromatography (eluent: EtOAc/petroleum ether = 1/4) with 63% isolated yield (35.3 mg). m. p. = 166-168°C. ^{1}H NMR (500 MHz, $CDCl_3$) δ 9.04 (d, *J* = 4.2 Hz, 1H), 8.81 (d, *J* = 5.2 Hz, 2H), 7.61 (d, *J* = 8.1 Hz, 1H), 7.52 (m, 4H), 7.42 (d, *J* = 4.3 Hz, 1H). ^{13}C NMR (126 MHz, $CDCl_3$) δ 158.2 (d, *J* = 257.3 Hz), 150.1, 150.0 (d, *J* = 1.0 Hz), 145.4, 145.4 (d, *J* = 3.0 Hz), 138.9 (d, *J* = 11.7 Hz), 127.4, 126.9 (d, *J* = 8.3 Hz), 124.1, 121.8, 120.7 (d, *J* = 4.8 Hz), 113.8 (d, *J* = 19.0 Hz). ^{19}F NMR (471 MHz, $CDCl_3$) δ -123.9. HRMS (ESI) *m/z:* [M + H] $^+$ calcd for $C_{14}H_9FN_2$: 225.0823, found: 225.0824.

8-Chloro-2-(pyridin-4-yl)quinoline (3na)

(Hey and Williams, 1950, Nunn and Schofield, 1952; Kouznetsov et al., 2012, 2017; Yamaguchi et al., 2016; Pang et al., 2017; Zhang et al., 2017a, 2017b; Roder et al., 2019) yellow oil was obtained by column chromatography (eluent: EtOAc/petroleum ether = 1/4) with 45% isolated yield (27 mg). ^{1}H NMR (500 MHz, $CDCl_3$) δ 8.79 (d, *J* = 5.3 Hz, 2H), 8.29 (d, *J* = 8.6 Hz, 1H), 8.15 (d, *J* = 6.1 Hz, 2H), 7.97 (d, *J* = 8.6 Hz, 1H), 7.87 (d, *J* = 7.5 Hz, 1H), 7.77 (d, *J* = 8.2 Hz, 1H), 7.48 (t, *J* = 7.8 Hz, 1H). ^{13}C NMR (126 MHz, $CDCl_3$) δ 154.6, 150.4, 144.4, 137.8, 134.4, 130.2, 127.2, 126.6, 121.7, 118.9.

8-Chloro-4-(pyridin-4-yl)quinoline (3na′)

yellow solid was obtained by column chromatography (eluent: EtOAc/petroleum ether = 1/4) with 44% isolated yield (26.5 mg). m. p. = 164-166°C. ^{1}H NMR (500 MHz, $CDCl_3$) δ 9.12 (d, *J* = 4.3 Hz, 1H), 8.81 (d, *J* = 4.1 Hz, 2H), 7.90 (d, *J* = 7.4 Hz, 1H), 7.74 (d, *J* = 8.4 Hz, 1H), 7.47 (t, *J* = 8.0 Hz, 1H), 7.43 (d, *J* = 4.9 Hz, 2H), 7.41 (d, *J* = 4.3 Hz, 1H). ^{13}C NMR (126 MHz, $CDCl_3$) δ 150.4, 150.1, 146.1, 145.5, 144.8, 134.2, 127.2, 127.0, 124.2, 124.2, 121.8. HRMS (ESI) *m/z:* [M + H] $^+$ calcd for $C_{14}H_9ClN_2$: 241.0527, found: 241.0522

[2,4′-bipyridine]-4-carbonitrile (4aa)

(Hey and Williams, 1950, Nunn and Schofield, 1952; Kouznetsov et al., 2012, 2017; Yamaguchi et al., 2016; Pang et al., 2017; Zhang et al., 2017a, 2017b; Roder et al., 2019) yellow solid was obtained by column chromatography (eluent: EtOAc/petroleum ether = 1/4) with 40% isolated yield (18.1 mg). m. p. = 199-201°C. ^{1}H NMR (500 MHz, $CDCl_3$) δ 8.94 (d, *J* = 4.9 Hz, 1H), 8.80 (d, *J* = 5.8 Hz, 2H), 8.03 (s, 1H), 7.91 (d, *J* = 5.9 Hz, 2H), 7.58 (d, *J* = 4.9 Hz, 1H). ^{13}C NMR (126 MHz, $CDCl_3$) δ 156.1, 151.1, 150.8, 144.2, 124.9, 122.3, 121.7, 120.9, 116.2.

2-(Pyridin-4-yl)quinazoline (3qa)

(Hey and Williams, 1950, Nunn and Schofield, 1952; Kouznetsov et al., 2012, 2017; Yamaguchi et al., 2016; Pang et al., 2017; Zhang et al., 2017a, 2017b; Roder et al., 2019) yellow solid was obtained by column chromatography (eluent: EtOAc/petroleum ether = 1/4) with 58% isolated yield (30.0 mg). m. p. = 128-130°C. ^{1}H NMR (500 MHz, $CDCl_3$) δ 9.43 (s, 1H), 8.88 (d, *J* = 5.1 Hz, 2H), 8.18 (d, *J* = 8.5 Hz, 1H), 8.05 (d, *J* = 8.5 Hz, 1H), 7.99 (t, *J* = 7.7 Hz, 1H), 7.71 (d, *J* = 5.9 Hz, 2H), 7.68 (d, *J* = 8.1 Hz, 1H). ^{13}C NMR (126 MHz, $CDCl_3$) δ 165.7, 154.6, 151.1, 150.0, 144.7, 134.2, 129.2, 128.4, 126.0, 124.2.

2-(Isoquinolin-1-yl)quinazoline (3qb)

yellow solid was obtained by column chromatography (eluent: EtOAc/petroleum ether = 1/4) with 69% isolated yield (44.4 mg). m. p. = 184-186°C. ^{1}H NMR (500 MHz, $CDCl_3$) δ 9.52 (s, 1H), 8.74 (d, *J* = 5.6 Hz, 1H), 8.19 (d, *J* = 8.5 Hz, 1H), 8.00 (m, 2H), 7.89 (m, 3H), 7.76 (t, *J* = 7.6 Hz, 1H), 7.60 (m, 2H). ^{13}C NMR (126 MHz, $CDCl_3$) δ 166.1, 155.5, 154.3, 151.3, 141.9, 136.9, 134.2, 130.7, 128.8, 128.1, 128.0, 127.3, 127.1, 127.0, 126.6, 124.2, 121.9. HRMS (ESI) *m/z:* [M + H] $^{+}$ calcd for $C_{17}H_{11}N_3$: 258.1026, found: 258.1026.

6-(Pyridin-4-yl)phenanthridine (3ra)

yellow oil was obtained by column chromatography (eluent: EtOAc/petroleum ether = 1/6) with 62% isolated yield (39.7 mg). ^{1}H NMR (500 MHz, $CDCl_3$) δ 8.84 (d, 2H), 8.73 (d, *J* = 8.3 Hz, 1H), 8.63 (d, *J* = 8.1 Hz, 1H), 8.24 (d, *J* = 6.9 Hz, 1H), 8.01 (d, *J* = 8.2 Hz, 1H), 7.90 (t, *J* = 7.7 Hz, 1H), 7.79 (t, *J* = 7.1 Hz, 1H), 7.73 (t, *J* = 7.6 Hz, 1H), 7.69 (d, *J* = 3.8 Hz, 2H), 7.65 (t, *J* = 7.1 Hz, 1H). ^{13}C NMR (126 MHz, $CDCl_3$) δ 158.4, 149.7, 147.6, 143.5, 133.5, 131.0, 130.4, 129.1, 127.9, 127.6, 127.5, 124.5, 124.4, 123.9, 122.5, 122.0. HRMS (ESI) *m/z:* [M + H] $^{+}$ calcd for $C_{18}H_{12}N_2$: 257.1073, found: 257.1075.

6-(Isoquinolin-1-yl)phenanthridine (3rb)

yellow oil was obtained by column chromatography (eluent: petroleum ether) with 70% isolated yield (53.6 mg). ^{1}H NMR (500 MHz, $CDCl_3$) δ 8.78 (m, 2H), 8.71 (d, *J* = 9.3 Hz, 1H), 8.27 (d, *J* = 6.7 Hz, 1H), 7.97 (d, *J* = 8.3 Hz, 1H), 7.89 (m, 2H), 7.81 (m, 3H), 7.71 (d, *J* = 8.2 Hz, 2H), 7.54 (t, *J* = 7.6 Hz, 1H), 7.46 (t, *J* = 7.2 Hz, 1H). ^{13}C NMR (126 MHz, $CDCl_3$) δ 158.6, 158.2, 143.5, 142.0, 136.9, 133.4, 130.9, 130.5, 130.5, 128.9, 128.4, 127.8, 127.6, 127.5, 127.4, 127.1, 127.00 125.8, 124.2, 122.1, 122.1, 121.2. HRMS (ESI) *m/z:* [M + H] $^{+}$ calcd for $C_{22}H_{14}N_2$: 307.1230, found: 307.1230.

9-(Pyridin-4-yl)acridine (3sa)

yellow oil was obtained by column chromatography (eluent: EtOAc/petroleum ether = 1/6) with 64% isolated yield (41.0 mg). ^{1}H NMR (500 MHz, $CDCl_3$) δ 8.81 (d, *J* = 5.4 Hz, 2H), 8.22 (d, *J* = 8.8 Hz, 2H), 7.79 (m, 2H), 7.51 (d, *J* = 8.7 Hz, 2H), 7.41 (m, 2H), 7.34 (d, *J* = 5.8 Hz, 2H). ^{13}C NMR (126 MHz, $CDCl_3$) δ 150.0, 148.6, 144.5, 143.5, 130.2, 129.8, 126.3, 125.8, 125.4, 124.1. HRMS (ESI) *m/z:* [M + H] $^{+}$ calcd for $C_{18}H_{12}N_2$: 257.1073, found: 257.1071.

9-(2-Fluoropyridin-4-yl)acridine (3sc)

yellow oil was obtained by column chromatography (eluent: EtOAc/petroleum ether = 1/6) with 51% isolated yield (35.9 mg). ^{1}H NMR (500 MHz, $CDCl_3$) δ 8.50 (d, *J* = 5.0 Hz, 1H), 8.32 (d, *J* = 8.8 Hz, 2H), 7.85 (m, 2H), 7.58 (d, *J* = 8.5 Hz, 2H), 7.53 (m, 2H), 7.31 (d, *J* = 4.9 Hz, 1H), 7.08 (s, 1H). ^{13}C NMR (126 MHz, $CDCl_3$) δ 163.9 (d, *J* = 241.6 Hz), 150.1 (d, *J* = 7.4 Hz), 148.5, 148.1 (d, *J* = 14.9 Hz), 142.2, 130.3, 129.9, 126.7, 125.5, 123.9, 123.3 (d, *J* = 4.7 Hz), 111.5 (d, *J* = 37.4 Hz). ^{19}F NMR (471 MHz, $CDCl_3$) δ -66.5. HRMS (ESI) *m/z:* [M + H] $^{+}$ calcd for $C_{18}H_{11}FN_2$: 275.0979, found: 275.0977.

9-(3-Chloropyridin-4-yl)acridine (3sd)

yellow oil was obtained by column chromatography (eluent: EtOAc/petroleum ether = 1/6) with 55% isolated yield (40.0 mg). ^{1}H NMR (500 MHz, $CDCl_3$) δ 8.92 (s, 1H), 8.76 (d, *J* = 4.8 Hz, 1H), 8.35 (d, *J* = 8.8 Hz, 2H), 7.83 (t, *J* = 7.0 Hz, 2H), 7.51 (t, *J* = 8.2 Hz, 2H), 7.45 (d, *J* = 8.5 Hz, 2H), 7.37 (d, *J* = 4.8 Hz, 1H). ^{13}C NMR (126 MHz, $CDCl_3$) δ 150.2, 147.8, 140.7, 137.0, 131.7, 130.4, 129.8, 126.8, 126.2, 125.3, 123.8, 99.9. HRMS (ESI) *m/z:* [M + H] $^{+}$ calcd for $C_{18}H_{11}ClN_2$: 291.0684, found: 291.0681.

9-(4-Methylpyridin-2-yl)acridine (3se)

yellow oil was obtained by column chromatography (eluent: EtOAc/petroleum ether = 1/6) with 70% isolated yield (47.3 mg). ^{1}H NMR (500 MHz, $CDCl_3$) δ 8.77 (d, *J* = 5.1 Hz, 1H), 8.29 (d, *J* = 8.8 Hz, 2H), 7.77 (t, *J* = 7.8 Hz, 2H), 7.65 (d, *J* = 8.7 Hz, 2H), 7.45 (t, *J* = 7.7 Hz, 2H), 7.37 (s, 1H), 7.33 (d, *J* = 5.0 Hz, 1H), 2.50 (s, 3H). ^{13}C NMR (126 MHz, $CDCl_3$) δ 155.3, 149.8, 148.8, 147.7, 144.9, 130.0, 129.6, 127.0, 126.2, 126.0, 124.7, 124.1, 29.7. HRMS (ESI) *m/z:* [M + H] $^{+}$ calcd for $C_{19}H_{14}N_2$: 271.1230, found: 271.1229.

methyl 2-(acridin-9-yl)isonicotinate (3sf)

yellow oil was obtained by column chromatography (eluent: EtOAc/petroleum ether = 1/6) with 71% isolated yield (55.8 mg). ^{1}H NMR (500 MHz, $CDCl_3$) δ 9.10 (d, *J* = 5.0 Hz, 1H), 8.34 (d, *J* = 8.8 Hz, 2H), 8.11 (s, 1H), 8.09 (d, *J* = 5.0 Hz, 1H), 7.80 (t, *J* = 7.2 Hz, 2H), 7.58 (d, *J* = 8.7 Hz, 2H), 7.48 (t, *J* = 7.0 Hz, 2H), 3.98 (d, *J* = 12.1 Hz, 3H), δ 3.99 (s, 1H). ^{13}C NMR (126 MHz, $CDCl_3$) δ 165.3, 156.6, 153.7, 151.1, 148.6, 138.0, 130.3, 129.5, 126.5, 125.8, 125.3, 124.5, 122.4, 52.9. HRMS (ESI) *m/z:* [M + H] $^+$ calcd for $C_{20}H_{14}N_2O_2$: 315.1128, found: 315.1126.

9-(4-(tert-butyl)pyridin-2-yl)acridine (3sg)

yellow oil was obtained by column chromatography (eluent: EtOAc/petroleum ether = 1/6) with 84% isolated yield (65.6 mg). ^{1}H NMR (500 MHz, $CDCl_3$) δ 8.82 (d, *J* = 5.3 Hz, 1H), 8.30 (d, *J* = 8.8 Hz, 2H), 7.78 (t, *J* = 7.4 Hz, 2H), 7.66 (d, *J* = 8.7 Hz, 2H), 7.54 (s, 1H), 7.50 (d, *J* = 5.4 Hz, 1H), 7.46 (t, *J* = 7.6 Hz, 2H), 1.40 (s, 7H). ^{13}C NMR (126 MHz, $CDCl_3$) δ 160.8, 155.1, 149.9, 148.8, 145.3, 130.0, 129.5, 126.2, 126.1, 124.7, 123.4, 120.2, 35.0, 30.6. HRMS (ESI) *m/z:* [M + H] $^+$ calcd for $C_{22}H_{20}N_2$: 313.1699, found: 313.1696.

9-(6-Methylpyridin-2-yl)acridine (3sh)

Yellow oil was obtained by column chromatography (eluent: EtOAc/petroleum ether = 1/6) with 62% isolated yield (41.9 mg). ^{1}H NMR (500 MHz, $CDCl_3$) δ 8.28 (d, *J* = 8.8 Hz, 2H), 7.85 (t, *J* = 7.7 Hz, 1H), 7.77 (t, *J* = 6.7 Hz, 2H), 7.65 (d, *J* = 8.7 Hz, 2H), 7.45 (t, *J* = 6.7 Hz, 2H), 7.38 (d, *J* = 7.8 Hz, 1H), 7.35 (d, *J* = 7.6 Hz, 1H), 2.72 (s, 1H). ^{13}C NMR (126 MHz, $CDCl_3$) δ 159.0, 154.8, 148.9, 144.9, 136.6, 129.9, 129.6, 126.3, 126.0, 124.7, 123.2, 122.7, 24.7. HRMS (ESI) *m/z:* [M + H] $^+$ calcd for $C_{19}H_{14}N_2$: 271.1230, found: 271. 1230.

9-(Isoquinolin-1-yl)acridine (3sb)

yellow oil was obtained by column chromatography (eluent: EtOAc/petroleum ether = 1/6) with 67% isolated yield (51.3 mg). ^{1}H NMR (500 MHz, $CDCl_3$) δ 8.83 (d, *J* = 5.7 Hz, 1H), 8.35 (d, *J* = 8.8 Hz, 2H), 8.01 (d, *J* = 8.3 Hz, 1H), 7.91 (d, *J* = 5.7 Hz, 1H), 7.77 (t, *J* = 6.5 Hz, 2H), 7.71 (t, *J* = 7.1 Hz, 1H), 7.37 (m, 5H), 7.20 (d, *J* = 8.4 Hz, 1H). ^{13}C NMR (126 MHz, $CDCl_3$) δ 157.0, 148.8, 143.3, 142.7, 136.2, 130.7, 130.1, 129.7, 128.5, 127.9, 127.1, 127.0, 126.2, 126.2, 125.4, 121.0. HRMS (ESI) *m/z:* [M + H] $^+$ calcd for $C_{22}H_{14}N_2$: 307.1230, found: 307.1229.

2-(Pyridin-2-yl)quinoline (3ai)

(Hey and Williams, 1950, Nunn and Schofield, 1952; Kouznetsov et al., 2012, 2017; Yamaguchi et al., 2016; Pang et al., 2017; Zhang et al., 2017a, 2017b; Roder et al., 2019) yellow solid was obtained by column chromatography (eluent: EtOAc/petroleum ether = 1/4) with 43% isolated yield (22.2 mg). m. p. = 93-95°C. ^{1}H NMR (500 MHz, $CDCl_3$) δ 8.75 (d, *J* = 4.6 Hz, 1H), 8.66 (d, *J* = 8.0 Hz, 1H), 8.56 (d, *J* = 8.6 Hz, 1H), 8.29 (d, *J* = 8.6 Hz, 1H), 8.19 (d, *J* = 8.5 Hz, 1H), 7.90 (m, 2H), 7.74 (t, *J* = 8.2 Hz, 1H), 7.56 (t, *J* = 7.5 Hz, 1H), 7.37 (t, 1H).^{13}C NMR (126 MHz, $CDCl_3$) δ 156.3, 156.1, 149.1, 147.9, 136.9, 136.8, 129.8, 129.5, 128.2, 127.6, 126.7, 124.0, 121.8, 118.9.

4-Dimethyl-2-(pyridin-2-yl)quinoline (3ei)

(Hey and Williams, 1950, Nunn and Schofield, 1952; Kouznetsov et al., 2012, 2017; Yamaguchi et al., 2016; Pang et al., 2017; Zhang et al., 2017a, 2017b; Roder et al., 2019) yellow oil was obtained by column chromatography (eluent: EtOAc/petroleum ether = 1/4) with 46% isolated yield (25.3 mg). ^{1}H NMR (500 MHz, $CDCl_3$) δ 8.74 (d, *J* = 4.1 Hz, 1H), 8.65 (d, *J* = 7.9 Hz, 1H), 8.40 (s, 1H), 8.19 (d, *J* = 8.5 Hz, 1H), 8.04 (d, *J* = 8.2 Hz, 1H), 7.88 (t, *J* = 7.7 Hz, 1H), 7.73 (t, *J* = 7.6 Hz, 1H), 7.58 (t, *J* = 7.5 Hz, 1H), 7.36 (t, *J* = 6.2 Hz, 1H), 2.80 (s, 3H). ^{13}C NMR (126 MHz, $CDCl_3$) δ 156.5, 155.6, 149.1, 147.8, 145.1, 137.0, 130.3, 129.2, 128.3, 126.5, 124.0, 123.8, 121.9, 119.5, 18.9.

4-Methyl-2-(4-methylpyridin-2-yl)quinoline (3ee)

yellow oil was obtained by column chromatography (eluent: EtOAc/petroleum ether = 1/4) with 72% isolated yield (42.2 mg). ^{1}H NMR (500 MHz, $CDCl_3$) δ 8.60 (d, *J* = 4.9 Hz, 1H), 8.47 (s, 1H), 8.39 (s, 1H), 8.19 (d, *J* = 8.4 Hz, 1H), 8.03 (d, *J* = 8.3 Hz, 1H), 7.73 (t, *J* = 7.6 Hz, 1H), 7.57 (t, *J* = 7.5 Hz, 1H), 7.19 (d, *J* = 4.6 Hz, 1H), 2.80 (s, 3H), 2.49 (s, 3H). ^{13}C NMR (126 MHz, $CDCl_3$) δ 156.2, 155.8, 148.9, 148.2, 147.7, 145.1, 130.2, 129.2, 128.2, 126.4, 125.0, 123.8, 122.6, 119.7, 29.7, 18.9. HRMS (ESI) *m/z:* [M + H] $^+$ calcd for $C_{16}H_{14}N_2$: 235.1230, found: 235.1229.

2-(4-(tert-butyl)pyridin-2-yl)-4-methylquinoline (3eg)

yellow oil was obtained by column chromatography (eluent: EtOAc/petroleum ether = 1/4) with 76% isolated yield (52.5 mg). ^{1}H NMR (500 MHz, $CDCl_3$) δ 8.65 (d, J = 5.8 Hz, 2H), 8.39 (s, 1H), 8.23 (d, J = 8.1 Hz, 1H), 8.03 (d, J = 8.1 Hz, 1H), 7.73 (t, J = 7.4 Hz, 1H), 7.57 (t, J = 7.3 Hz, 1H), 7.37 (d, J = 3.7 Hz, 1H), 2.80 (s, 3H), 1.44 (s, 9H). ^{13}C NMR (126 MHz, $CDCl_3$) δ 161.2, 156.2, 155.9, 148.9, 147.6, 145.1, 130.3, 129.2, 128.2, 126.4, 123.7, 121.3, 119.8, 118.9, 30.6, 29.7, 18.9. HRMS (ESI) *m/z:* $[M + H]^+$ calcd for $C_{19}H_{20}N_2$: 277.1699, found: 277.1699.

4-Methyl-2-(6-methylpyridin-2-yl)quinoline (3eh)

(Hey and Williams, 1950, Nunn and Schofield, 1952; Kouznetsov et al., 2012, 2017; Yamaguchi et al., 2016; Pang et al., 2017; Zhang et al., 2017a, 2017b; Roder et al., 2019) yellow oil was obtained by column chromatography (eluent: EtOAc/petroleum ether = 1/4) with 63% isolated yield (36.9 mg). ^{1}H NMR (500 MHz, $CDCl_3$) δ 8.41 (d, J = 5.7 Hz, 2H), 8.18 (d, J = 8.4 Hz, 1H), 8.02 (d, J = 8.3 Hz, 1H), 7.77–7.70 (m, 2H), 7.56 (t, J = 7.6 Hz, 1H), 7.22 (d, J = 7.6 Hz, 1H), 2.80 (s, 3H), 2.69 (s, 3H). ^{13}C NMR (126 MHz, $CDCl_3$) δ 157.8, 156.0, 155.9, 147.8, 144.9, 137.1, 130.3, 129.1, 128.2, 123.7, 123.5, 119.6, 118.9, 29.7, 18.9.

4-Methyl-2,2′-biquinoline (3eb)

(Hey and Williams, 1950, Nunn and Schofield, 1952; Kouznetsov et al., 2012, 2017; Yamaguchi et al., 2016; Pang et al., 2017; Zhang et al., 2017a, 2017b; Roder et al., 2019) yellow oil was obtained by column chromatography (eluent: EtOAc/petroleum ether = 1/4) with 54% isolated yield (36.5 mg). ^{1}H NMR (500 MHz, $CDCl_3$) δ 8.85 (d, J = 8.6 Hz, 1H), 8.69 (s, 1H), 8.33 (d, J = 8.6 Hz, 1H), 8.25 (d, J = 8.4 Hz, 2H), 8.06 (d, J = 8.3 Hz, 1H), 7.89 (d, J = 8.1 Hz, 1H), 7.79 (m, 2H), 7.63 (m, 2H), 2.86 (s, 3H). ^{13}C NMR (126 MHz, $CDCl_3$) δ 154.8, 147.9, 141.7, 140.8, 136.8, 135.7, 131.3, 130.4, 129.8, 129.5, 129.3, 128.4, 127.7, 126.9, 126.7, 123.8, 119.9, 119.5, 19.0.